(2)

DNA-TR-81-327

CURRENTS INDUCED ON UNINSULATED WIRES WITH FINITE CONDUCTIVITY

G. Sherman
Mission Research Corporation
P.O. Drawer 719
Santa Barbara, CA 93102

1 November 1983

Technical Report

CONTRACT No. DNA 001-81-C-0175

THIS WORK WAS SPONSORED BY THE DEFENSE NUCLEAR AGENCY
UNDER RDT&E RMSS CODE B326081466 X99QAXVD00011 H2590D.

Prepared for
Director
DEFENSE NUCLEAR AGENCY
Washington, DC 20305

Destroy this report when it is no longer needed. Do not return to sender.

PLEASE NOTIFY THE DEFENSE NUCLEAR AGENCY, ATTN: STTI, WASHINGTON, D.C. 20305, IF YOUR ADDRESS IS INCORRECT, IF YOU WISH TO BE DELETED FROM THE DISTRIBUTION LIST, OR IF THE ADDRESSEE IS NO LONGER EMPLOYED BY YOUR ORGANIZATION.

UNCLASSIFIED

SECURITY CLASSIFICATION OF THIS PAGE *(When Data Entered)*

REPORT DOCUMENTATION PAGE		READ INSTRUCTIONS BEFORE COMPLETING FORM
1. REPORT NUMBER DNA-TR-81-327	2. GOVT ACCESSION NO. AD-A152 191	3. RECIPIENT'S CATALOG NUMBER
4. TITLE *(and Subtitle)* CURRENTS INDUCED ON UNINSULATED WIRES WITH FINITE CONDUCTIVITY		5. TYPE OF REPORT & PERIOD COVERED Technical Report 6. PERFORMING ORG. REPORT NUMBER MRC-R-796
7. AUTHOR(s) George Sherman		8. CONTRACT OR GRANT NUMBER(s) DNA 001-81-C-0175
9. PERFORMING ORGANIZATION NAME AND ADDRESS Mission Research Corporation PO Drawer 719 Santa Barbara, CA 93102		10. PROGRAM ELEMENT, PROJECT, TASK AREA & WORK UNIT NUMBERS Task X99QAXVD-00011
11. CONTROLLING OFFICE NAME AND ADDRESS Director Defense Nuclear Agency Washington, DC 20305-1000		12. REPORT DATE 1 November 1983 13. NUMBER OF PAGES 78
14. MONITORING AGENCY NAME & ADDRESS*(if different from Controlling Office)*		15. SECURITY CLASS *(of this report)* UNCLASSIFIED 15a. DECLASSIFICATION DOWNGRADING SCHEDULE N/A since UNCLASSIFIED

16. DISTRIBUTION STATEMENT *(of this Report)*

Approved for public release; distribution is unlimited.

17. DISTRIBUTION STATEMENT *(of the abstract entered in Block 20, if different from Report)*

18. SUPPLEMENTARY NOTES

This work was sponsored by the Defense Nuclear Agency under RDT&E RMSS Code B326081466 X99QAXVD00011 H2590D.

19. KEY WORDS *(Continue on reverse side if necessary and identify by block number)*

Source Region EMP Coupling
Buried Cables
Transmission Line Theory
Electronmagnetic Scattering
EMP Coupling to Power Systems
EMP Coupling to Communications Lines

20. ABSTRACT *(Continue on reverse side if necessary and identify by block number)*

Calculations of the source region EMP response of very long buried and elevated cables have generally been performed using transmission-line theory. That theory is useful when the response is dominated by an approximately TEM mode. Although an uninsulated wire supports such a mode, it is very difficult to excite. Other waves may dominate the response, invalidating the application of transmission-line theory.

This study analyzes the response of an infinitely long, uninsulated

DD FORM 1 JAN 73 1473 EDITION OF 1 NOV 65 IS OBSOLETE

UNCLASSIFIED

SECURITY CLASSIFICATION OF THIS PAGE *(When Data Entered)*

20. ABSTRACT (Continued)

wire with finite conductivity in a homogeneous material to a monochromatic voltage-generating source localized near the wire. Using Fourier techniques, an exact integral representation of the current induced on the wire is obtained by solving the full electromagnetic scattering problem. The integral is then expressed using contour integration as the sum of pole residues and an integral around a branch cut. The residues represent the contributions of TM modes of the wire. All of these modes damp out immediately except one, known as the principal mode. The principal mode is approximately TEM and hence can be treated by transmission-line theory. The branch-cut integral represents the contribution of an electromagnetic wave (known as a space wave) that radiates out into space. The space-wave cannot be treated by standard transmission-line theory.

Numerical comparison of the magnitudes of the space-wave and the principal-mode contributions to the current for representative frequencies and wire resistances shows that the wire response is totally dominated by the space wave. Hence, standard transmission-line theory is not useful. Moreover, the results show that theory based on a perfect-conductor model of the wire is not very useful either. The current in the resistive wire is reduced by a substantial amount (from the perfect-conductor result) that is nearly independent of distance from the source over a very long range along the wire.

PREFACE

I am pleased to express my appreciation to Dr. James Gilbert for guidance on all aspects of this work. Special thanks are due to Bob Marks for his willingness to teach me what I needed to know in order to conduct the numerical portion of this study.

TABLE OF CONTENTS

LIST OF ILLUSTRATIONS

LIST OF TABLES

SECTION 1
INTRODUCTION

Calculations of the source region EMP response of very long buried and elevated cables have generally been performed by the use of the transmission-line approximation to the full electromagnetic scattering problem. (For examples, see References 1-2.) That approximation is useful when the response is dominated by an approximately transverse magnetic and transverse electric wave that is guided along the cable (a TEM mode). Usually, if a guiding structure supports a TEM mode, that mode dominates the response of the structure and the transmission-line theory applies. This appears to be the case with insulated antennas and wires since transmission-line theory predicts their response very accurately. The opposite situation exists, however, with a bare wire in the soil or air. Although such a wire supports a guided wave that is approximately a TEM mode, it is very difficult to excite. Indeed, if the wire were a perfect conductor, an infinite amount of energy would be required to excite the TEM mode.

The response of a perfectly conducting wire to a delta-function voltage generator on the wire was investigated in Reference 3. It was found that the results could be described by equations similar to transmission-line theory far from the source only if the inductance term was taken to be a function of distance from the source. The reason for this behavior is that the source does not generate any modes in the wire. Instead, it generates a wave known as a space wave that radiates out into space. The transmission-line equations do not apply to such waves.

The situation is much more complicated when the wire has finite resistance. In that case, the source can excite both a space wave and electromagnetic modes. One of those modes is approximately a TEM mode that can be treated by transmission-line theory. The only way to determine the relative importance of these various waves is to solve the full electromagnetic scattering problem. This is the purpose of the present study.

In this report, the coupling to an infinitely long, finitely conducting wire in homogeneous material is examined. An exact integral expression is obtained for the current generated in the wire by a voltage-generating source localized on the wire. The contributions of the space wave and the individual modes are isolated by applying contour-integration techniques. The contribution of the space wave arises as a branch-cut integral and the contributions of the various modes rise as residues of poles. Both the branch-cut integral and the residues are calculated numerically to compare their relative importance. In addition, analytic approximations for the space-wave current are obtained for points very near and very far from the source.

Numerical calculations were made for highly conducting lines (where the results reduced to those obtained in Reference 3) and for lines with resistances representative of buried communication and power systems. It was found that the TEM-type mode is not excited in wires with typical resistances at the frequencies of interest. Hence, the space wave is the dominant contributor to the current in these wires and consequently, standard transmission-line theory is not applicable. Moreover, it was found that, with representative resistances, the current produced is quite different from the current that would be produced on a perfectly conducting wire.

SECTION 2
INTEGRAL REPRESENTATION OF THE CURRENT

The problem of the current excited by a delta-function voltage generator on the surface of a straight wire has been treated in the case of a perfectly conducting wire by specifying the boundary value[3,4]

$$E_z = V_0\delta(z)$$

on the surface of the wire where E_z is the component of the electric field in the direction of the wire.* When the wire has finite conductivity, however, we cannot specify the value of the field anywhere in finite space. The problem is best treated as a scattering problem with a specified field $\underline{E}^i$ incident on the wire generating a scattered field $\underline{E}^s$ that is determined by the boundary conditions at the surface of the wire. The incident field is the field radiated by the generator if the wire is not present. Our first task, then is to determine that field.

In a material with finite or zero conductivity, a voltage generator produces a discontinuity in the electric field across the generator. The magnetic field can be continuous. In this study, the generator is specified to have these properties in such a way that the current it produces in the wire reduces, in the limit of infinite wire conductivity, to the result already known for the current produced by a voltage generator on a perfect conductor. The same generator has been applied by Wait[5] and by Wait and Hill[6] to study waves produced on cylindrical rods. (Those

---

* This problem was introduced into the EMP literature in Reference 3. It has a long history in the antenna-theory literature. See Reference 4 and the references therein.

studies differ from ours in that they apply an approximate boundary condition at the rod surface). The generator can be thought of as a toroid with very large current in a wire very tightly wound around a circular ring that encircles the wire. It can be modeled mathematically by a ring of magnetic current. We take the ring to lie in the plane $z = 0$ and to have radius b which is larger that the radius a of the wire. Later, we set $b = a$ to put the source on the wire.

Consider a monochromatic electromagnetic field with angular frequency ω in an isotropic homogeneous material. It can be expressed in terms of axial Hertz vectors in the form[7]

$$\underline{E}(r,\phi,z)=\nabla x\nabla x[U(r,\phi,z)\hat{1}_z] + i\omega\mu\nabla x[V(r,\phi,z)\hat{1}_z], \qquad (1a)$$

$$\underline{H}(r,\phi,z)=\nabla x[\eta U(r,\phi,z)\hat{1}_z]+\nabla x\nabla x[V(r,\phi,z)\hat{1}_z] \qquad (1b)$$

in SI units where the scalar potentials satisfy the inhomogeneous Helmholtz equation

$$(\nabla^2+k^2)\ U(r,\phi,z) = f_U(r,\phi,z)\ , \qquad (2a)$$

$$(\nabla^2+k^2)\ V(r,\phi,z) = f_V(r,\phi,z) \qquad (2b)$$

with source functions f_U and f_V that are nonzero only on sources or on boundaries separating different materials. The time behavior $e^{-i\omega t}$ has been suppressed in (1) and (2) and k and η are defined by

$$k^2 = i\mu\omega\eta\ , \qquad (3)$$

$$\eta = \sigma - i\omega\varepsilon \ , \tag{4}$$

where μ, ε, σ are respectively the permeability, permittivity and conductivity of the medium. We apply the cylindrical coordinate system illustrated in Figure 1.

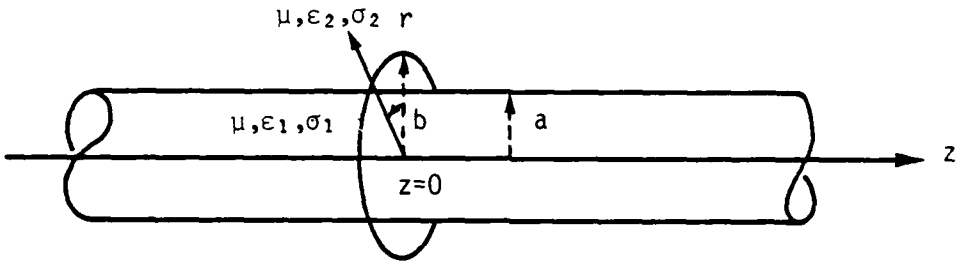

Figure 1. Magnetic current loop around a wire.

It follows from (1) that the axial components of the fields are given by

$$E_z(r,\phi,z) = (k^2 + \frac{\partial^2}{\partial z^2})\ U(r,\phi,z) \ , \tag{5}$$

$$H_z(r,\phi,z) = (k^2 + \frac{\partial^2}{\partial z^2})\ V(r,\phi,z). \tag{6}$$

Since the generator produces an axial electric field but no axial magnetic field, we assume that it is a source of the potential U but not of potential V. Since the scattering by the wire does not introduce any axial magnetic field either, we take V to be zero for both incident and

scattered fields. Moreover, from the symmetry of the problem, the potential $U(r,\phi,z)$ is independent of ϕ. For such fields, (1) reduce to

$$E_r(r,z) = \frac{\partial^2 U(r,z)}{\partial r \partial z} \ , \tag{7a}$$

$$E_\phi(r,z) = 0 \ , \tag{7b}$$

$$E_z(r,z) = (k^2 + \frac{\partial^2}{\partial z^2}) \ U(r,z) \ , \tag{7c}$$

$$H_r(r,z) = 0 \ , \tag{7d}$$

$$H_\phi(r,z) = -\eta \ \frac{\partial U(r,z)}{\partial r} \ , \tag{7e}$$

$$H_z(r,z) = 0 \tag{7f}$$

and (2a) reduces to

$$[\frac{1}{r} \frac{\partial}{\partial r} (r \frac{\partial}{\partial r}) + \frac{\partial^2}{\partial z^2} + k^2] \ U(r,z) = f_U(r,z) \ . \tag{8}$$

We now Fourier transform (7) and (8) with respect to z using the conventions

$$\tilde{A}(h) = \int_{-\infty}^{\infty} A(z) e^{-ihz} dz \ , \tag{9a}$$

$$A(z) = \frac{1}{2\pi} \int_{-\infty}^{\infty} \tilde{A}(h) e^{ihz} dh \ , \tag{9b}$$

to obtain (for the nonzero components)

$$\tilde{E}_r(r,h) = ih \frac{\partial \tilde{U}(r,h)}{\partial r} , \tag{10a}$$

$$\tilde{E}_z(r,h) = \alpha^2 \tilde{U}(r,h) , \tag{10b}$$

$$\tilde{H}_\phi(r,h) = -\eta \frac{\partial \tilde{U}(r,h)}{\partial r} \tag{10c}$$

$$[\frac{1}{r} \frac{\partial}{\partial r} (r \frac{\partial}{\partial r}) + \alpha^2] \tilde{U}(r,h) = \tilde{f}_U(r,h) , \tag{11}$$

where*

$$\alpha = \sqrt{k^2-h^2} . \tag{12}$$

We are now ready to solve for the field radiated by the generator without the presence of the wire. We use a superscript i for this field to indicate that it is the incident field in the scattering problem. A subscript 2 is used on the material parameters ϵ and σ and the corresponding quantities k, η, α defined in (3), (4), (12) to distinguish them from the same quantities within the wire which are indicated with subscript 1.

Since the source function for the potential $U^i(r,z)$ is zero everywhere except on the ring of radius b in the plane z=0, we have

$$f_U(r,z) = \frac{K}{r}\delta(r-b)\delta(z) , \tag{13a}$$

* For real h, the branch of the square root in (12) is chosen so that the imaginary part of α is positive or zero. The branch used for complex h is defined later.

and therefore have

$$\tilde{f}_U(r,h) = \frac{K}{r}\,\delta(r-b) \quad . \tag{13b}$$

Hence, for $r \neq b$, (11) is Bessel's equation of order zero with solutions

$$\tilde{U}^i(r,h) = C_1 H_0^{(1)}(\alpha_2 r) \text{ for } r>b \ , \tag{14a}$$

$$\tilde{U}^i(r,h) = C_2 J_0(\alpha_2 r) \text{ for } r<b \ , \tag{14b}$$

where the Hankel function in (14a) was chosen to insure outgoing waves at $r=\infty$ for positive α_2 and the Bessel function in (14b) was chosen to insure a finite result at $r=0$.

The ratio of the constants in (14) can be determined by requiring the continuity of $\tilde{H}_\phi(r,h)$ across $r=b$. According to (10c), this means that the r derivative of $\tilde{U}(r,h)$ must be continuous. Since the derivatives of the Hankel and Bessel functions with respect to their argument* satisfy[8]

$$\dot{H}_0^{(1)}(\alpha r) = -H_1^{(1)}(\alpha r) \ , \tag{15a}$$

$$\dot{J}_0(\alpha r) = -J_1(\alpha r) \ , \tag{15b}$$

we find

$$\frac{C_2}{C_1} = \frac{H_1^{(1)}(\alpha_2 b)}{J_1(\alpha_2 b)} \ . \tag{16}$$

---

* We use a dot over a function to indicate its derivative with respect to its argument.

Hence, (14) can be written

$$\tilde{U}^i(r,h) = C_0 J_1(\alpha_2 b)\, H_0^{(1)}(\alpha_2 r) \text{ for } r>b\ , \tag{17a}$$

$$\tilde{U}^i(r,h) = C_0 H_1^{(1)}(\alpha_2 b)\, J_0(\alpha_2 r) \text{ for } r<b. \tag{17b}$$

We can solve for the constant C_0 in terms of the discontinuity in $\tilde{U}^i(r,h)$ across r=b, but that is unnecessary. We determine it later in terms of the voltage V_0 across the generator. Also, we could now assemble the expressions for the incident electromagnetic field, but again, there is no point in doing so. It is most convenient to solve the scattering problem in terms of the potentials in Fourier space.

To that end, consider an infinitely long straight wire with circular cross section of radius a. The axis of the wire lies along the z axis. The permittivity and conductivity are ε_1 and σ_1 respectively in the wire and ε_2 and σ_2 outside the wire. The permeability is taken to be μ in both materials. We take the radius b of the generator to be slightly larger than a so that its field is incident on the wire from the outside. After solving the scattering problem, we can let $b \to a$ so that the generator is on the surface of the wire. The geometry is shown in Figure 1.

The incident field excites a scattered field with potential function $U^S(r,z)$ that propagates outward away from the wire in the outer material. The total field inside the wire has potential function $U^W(r,z)$. Both $U^S(r,z)$ and $U^W(r,z)$ satisfy the Helmholtz equation (2a) with $f_U=0$, and with k replaced by k_1 in the inner material and by

k_2 in the outer material. Hence, the Fourier transforms $\tilde{U}^s(r,h)$ and $\tilde{U}^w(r,h)$ of $U^s(r,z)$ and $U^w(r,z)$ respectively satisfy Bessel's equation with α defined in (12) replaced by $\alpha_1 = \sqrt{k_1^2 - h^2}$ in the wire and $\alpha_2 = \sqrt{k_2^2 - h^2}$ outside the wire. Hence, we must have

$$\tilde{U}^s(r,h) = AH_0^{(1)}(\alpha_2 r) \text{ for } r \geq a \ , \tag{18a}$$

$$\tilde{U}^w(r,h) = BJ_0(\alpha_1 r) \text{ for } r \leq a \ , \tag{18b}$$

where the particular solutions to Bessel equations were chosen in the same way as in (14).

The constants A and B in (18) can be determined by applying the boundary conditions that the tangential components of the electric and magnetic fields must be continuous at the surface of the wire. According to (10), this means that $\alpha^2\tilde{U}(r,h)$ and $\eta\frac{\partial\tilde{U}(r,h)}{\partial r}$ must be continuous there, where $\tilde{U}(r, h)$ is the Fourier transform of the total field. Outside the wire, $\tilde{U}(r, h)$ is $\tilde{U}^i(r,h) + \tilde{U}^s(r,h)$ whereas inside the wire it is $\tilde{U}^w(r,h)$. Hence, with the use of (17b) and (18), the boundary conditions become

$$C_0\alpha_2^2 H_1^{(1)}(\alpha_2 b)J_0(\alpha_2 a)+A\alpha_2^2 H_0^{(1)}(\alpha_2 a) = B\alpha_1^2 J_0(\alpha_1 a) \ , \tag{19a}$$

$$C_0\eta_2 H_1^{(1)}(\alpha_2 b)\alpha_2 \dot{J}_0(\alpha_2 a)+A\eta_2\alpha_2 \dot{H}_0^{(1)}(\alpha_2 a) = B\eta_1\alpha_1 \dot{J}_0(\alpha_1 a). \tag{19b}$$

With the application of (15), (19) becomes

$$A\alpha_2^2 H_0^{(1)}(\alpha_2 a)-B\alpha_1^2 J_0(\alpha_1 a) = -C_0\alpha_2^2 H_1^{(1)}(\alpha_2 b)J_0(\alpha_2 a) \ , \tag{20a}$$

$$-An_2\alpha_2 H_1^{(1)}(\alpha_2 a) + Bn_1\alpha_1 J_1(\alpha_1 a) = C_0 n_2\alpha_2 H_1^{(1)}(\alpha_2 b)J_1(\alpha_2 a). \quad (20b)$$

Solution of this pair of simultaneous linear equations yields

$$A = -C_0 H_1^{(1)}(\alpha_2 b)\,\frac{n_1\alpha_2 J_0(\alpha_2 a)J_1(\alpha_1 a) - \alpha_1 J_1(\alpha_2 a)J_0(\alpha_1 a)n_2}{\alpha_2 n_1 H_0^{(1)}(\alpha_2 a)J_1(\alpha_1 a) - \alpha_1 n_2 H_1^{(1)}(\alpha_2 a)J_0(\alpha_1 a)}\,, \quad (21a)$$

$$B = -C_0 n_2\,\frac{\alpha_2^2}{\alpha_1}\,H_1^{(1)}(\alpha_2 b)\,\frac{H_1^{(1)}(\alpha_2 a)J_0(\alpha_2 a) - H_0^{(1)}(\alpha_2 a)J_1(\alpha_2 a)}{\alpha_2 n_1 H_0^{(1)}(\alpha_2 a)J_1(\alpha_1 a) - \alpha_1 n_2 H_1^{(1)}(\alpha_2 a)J_0(\alpha_1 a)}\,. \quad (21b)$$

The numerator in (21b) is a Wronskian known to satisfy[9]

$$H_1^{(1)}(Z)J_0(Z) - H_0^{(1)}(Z)J_1(Z) = \frac{2}{\pi i Z}\,. \quad (22)$$

Hence, (21b) becomes

$$B = -\frac{2C_0\alpha_2 n_2}{\pi i\alpha_1 a}\,\frac{H_1^{(1)}(\alpha_2 b)}{\alpha_2 n_1 H_0^{(1)}(\alpha_2 a)J_1(\alpha_1 a) - \alpha_1 n_2 H_1^{(1)}(\alpha_2 a)J_0(\alpha_1 a)}\,. \quad (23)$$

According to (3) and (4), $n_2/n_1 = k_2^2/k_1^2$. Hence, (23) can be rewritten

$$B = -\frac{2C_0\alpha_2 k_2^2}{\pi i\alpha_1 a}\,\frac{H_1^{(1)}(\alpha_2 b)}{\alpha_2 k_1^2 H_0^{(1)}(\alpha_2 a)J_1(\alpha_1 a) - \alpha_1 k_2^2 H_1^{(1)}(\alpha_2 a)J_0(\alpha_1 a)}\,. \quad (24)$$

We now have everything we need to calculate all field quantities. Since our primary interest is in the current generated in the wire,

we will concentrate on the field inside the wire. From (18b) and (24), the Fourier transform of the potential of the total field inside the wire is

$$\tilde{U}^W(r,h) = -\frac{2C_0\alpha_2 k_2^2}{\pi i \alpha_1 a} \frac{H_1^{(1)}(\alpha_2 b) J_0(\alpha_1 r)}{\alpha_2 k_1^2 H_0^{(1)}(\alpha_2 a) J_1(\alpha_1 a) - \alpha_1 k_2^2 H_1^{(1)}(\alpha_2 a) J_0(\alpha_1 a)}$$

for $r \leq a$. (25)

The Fourier transform of the z component of the current density satisfies

$$\tilde{J}_z(r,h) = \sigma_1 \tilde{E}_z^W(r,h) = \alpha_1^2 \sigma_1 \tilde{U}^W(r,h) \tag{26}$$

and the Fourier transform of the total current flowing along the wire is the integral of $\tilde{J}(r,h)$ over the cross section of the wire

$$\tilde{I}(h) = 2\pi \int_0^a \tilde{J}_z(r,h)\, r dr. \tag{27}$$

Hence, by combining (25) - (27) and employing[10]

$$\int_0^a r J_0(\alpha_1 r) dr = \frac{r}{\alpha_1} J_1(\alpha_1 r) \Big|_0^a = \frac{a}{\alpha_1} J_1(\alpha_1 a) , \tag{28}$$

we obtain

$$\tilde{I}(h) = -\frac{4C_0\alpha_2 k_2^2 \sigma_1}{i} \frac{H_1^{(1)}(\alpha_2 b)\, J_1(\alpha_1 a)}{\alpha_2 k_1^2 H_0^{(1)}(\alpha_2 a) J_1(\alpha_1 a) - \alpha_1 k_2^2 H_1^{(1)}(\alpha_2 a) J_0(\alpha_1 a)} .$$

(29)

The desired integral expression for the total current I(z) flowing along the wire follows immediately if we take the inverse Fourier transform of (29) according to (9b). The result is

$$I(z) = -\frac{2k_2^2\sigma_1}{\pi i}\int_{-\infty}^{\infty}\frac{C_0\alpha_2 H_1^{(1)}(\alpha_2 b)J_1(\alpha_1 a)e^{ihz}}{\alpha_2 k_1^2 H_0^{(1)}(\alpha_2 a)J_1(\alpha_1 a)-\alpha_1 k_2^2 H_1^{(1)}(\alpha_2 a)J_0(\alpha_1 a)}\,dh\ . \tag{30}$$

The expression in (30) is similar to the formula applied by Wait and Hill[6] to treat the current generated on a metallic rod by a magnetic ring current. Their formula was derived[5] by assuming an approximate impedance-type boundary condition without specifying what the impedance actually is. Such boundary conditions are known to be useful when one of the materials has a large but finite conductivity.[5] If we replace the factor σ_1 outside the integral sign in (30) by η_1 so that I(Z) includes the displacement current or if we approximate k_1^2 in the first term in the denominator by $i\mu\omega\sigma_1$, then (30) becomes equivalent to the formula in Wait and Hill[6] if we take the series impedance of the wire to be

$$Z_s = \frac{\alpha_1 J_0(\alpha_1 a)}{2\pi a\eta_1 J_1(\alpha_1 a)} \tag{31}$$

and our constant C_0 to be

$$C_0 = \frac{\pi i b}{2\alpha_2}K\ , \tag{32}$$

where K is the strength of the magnetic ring current. The expression for the series impedance of a wire given in (31) is one that has been used in the EMP literature when the definition of Z_s is taken to be $E_z(a,z)/I(z)$ for axisymmetric TM fields.[2]

We can express C_0 in terms of the voltage V_0 across the voltage generator by relating (30) to the known result for the current produced on a perfect conductor by a voltage generator. To that end, we let b=a so that the source is on the wire, and consider (30) in the limit as $\sigma_1 \to \infty$. In that limit, the second term in the denominator in (30) is negligible compared to the first and $\sigma_1/k_1^2 \to 1/(i\mu\omega)$. Hence, we have

$$\lim_{\sigma_1 \to \infty} I(z) = \frac{2k_2^2}{\pi\mu\omega} \int_{-\infty}^{\infty} \frac{C_0 H_1^{(1)}(\alpha_2 a)}{H_0^{(1)}(\alpha_2 a)} e^{ihz} dh. \tag{33}$$

This corresponds to the known expression in this limit[3,4] if we take

$$C_0 = \frac{\pi i}{2\alpha_2} a V_0 . \tag{34}$$

Comparison of (34) and (32) shows that the magnetic ring current of strength K is a voltage generator of strength V_0.

The current can now be expressed terms of the voltage V_0 even when the generator is not on the wire by changing a to b in (34) and substituting into (30)

$$I(z) = - V_0 k_2^2 \sigma_1 b \int_{-\infty}^{\infty} \frac{H_1^{(1)}(\alpha_2 b) J_1(\alpha_1 a) e^{ihz}}{\alpha_2 k_1^2 H_0^{(1)}(\alpha_2 a) J_1(\alpha_1 a) - \alpha_1 k_2^2 H_1^{(1)}(\alpha_2 a) J_0(\alpha_1 a)} dh . \tag{35}$$

Equation (35) presents an exact integral expression for the total current generated by the source as a function of distance along the wire. Unfortunately, it is difficult to determine the properties of the current from the integral in its present form. In the next section, we transform the integral into a form which is more amenable to asymptotic and numerical analysis. Moreover, the transformed result provides new insight into the physics of the current flow.

SECTION 3
TRANSFORMATION OF THE CURRENT INTEGRAL

In this section, we transform the integral in (35) for positive z by completing the contour of integration in the upper half plane and applying Cauchy's theorem of the residues.* To that end, we rewrite (35) in the form

$$I(z) = -V_0 k_2^2 \sigma_1 b P(z) \ , \tag{36}$$

where

$$P(z) = \int_{-\infty}^{\infty} L(h)dh \ , \tag{37}$$

$$L(h) = \frac{H_1^{(1)}(\alpha_2 b)J_1(\alpha_1 a)e^{ihz}}{\alpha_1 k_2^2 H_1^{(1)}(\alpha_2 a)J_0(\alpha_1 a) - \alpha_2 k_1^2 H_0^{(1)}(\alpha_2 a)J_1(\alpha_1 a)} \ , \tag{38}$$

and investigate the analytic properties of the integrand L(h) in the upper half of the complex h plane.

---

* We apply a procedure that is standard in the theory of guided waves. E.g., see Reference 11.

3.1 MULTIVALUED FUNCTIONS AND BRANCH CUTS

The integrand $L(h)$ involves multivalued functions α_1, α_2, and $H_0^{(1)}(Z)$ which must be made single valued by specifying the branches to be used. For α_1, we choose the branch cut to be the curve* in the complex h plane where** $\alpha_1''=0$. This branch cut is shown as a dashed line ending at the branch points $h=\pm k_1$ in Figure 2. We take $\alpha_1'' \geq 0$ on the top Riemann sheet and $\alpha_1'' \leq 0$ on the bottom Riemann sheet. For α_2, we take the branch cut*** to be the vertical lines terminating at the branch points $h=\pm k_2$ that are shown in Figure 2 as wiggly lines. The dashed curves terminating at these branch points are curves where $\alpha_2''=0$. In the shaded region between each of these curves and its closest branch cut, α_2'' is negative on the top Riemann sheet. Elsewhere in the complex plane, α_2'' is positive on the top Riemann sheet. It follows from these definitions and the original definition of α given in (12) for real h, that the integration contour in (37) is on the top Riemann sheets of both α_1 and α_2.

For the Hankel function $H_0^{(1)}(Z)$, we choose the branch cut to lie along the negative half of the imaginary axis in the complex Z plane. This differs from the standard definition of $H_0^{(1)}(Z)$ which uses the negative real axis. Our branch of the Hankel function is chosen so that it is equal to the standard Hankel function in the upper half of the Z plane. The branch cut for the Hankel function $H_0^{(\cdot)}(\alpha_2 a)$ occurs only on the lower Riemann sheet of α_2. On that Riemann sheet, it lies along the dotted curve shown in Figure 2.

---

* This branch cut is frequently called the Sommerfield or the fundamental cut. See Reference 11 for a discussion of the characteristics.

** We use the notation that Z' is the real part and Z" is the imaginary part of any complex quantity Z.

*** This branch cut is called the vertical branch cut.

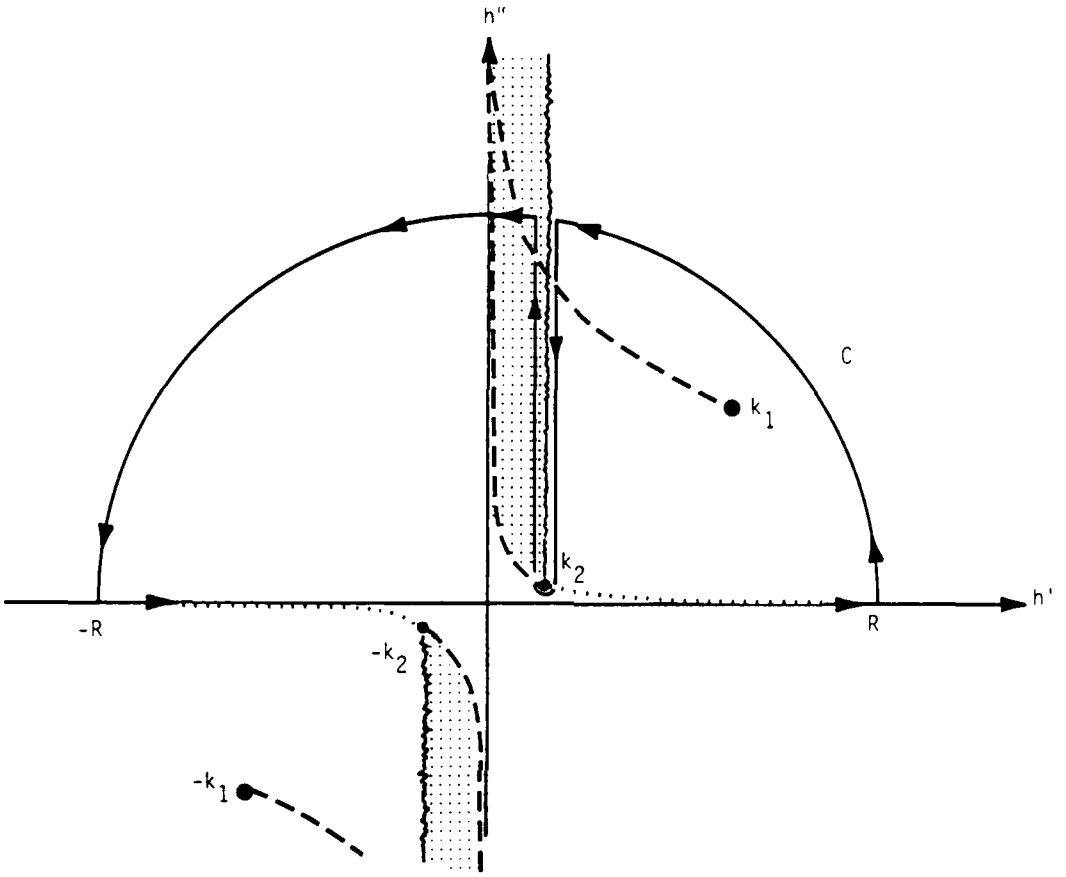

Figure 2. Complex h plane.

Even though the point $h=k_1$ is a branch point of α_1, it turns out that it is not a branch point of the integrand L(h). To see that, we temporarily write L(h) as $L(h,\alpha_1)$ and examine the value of the integrand on the opposite Riemann sheet of α_1, by evaluating $L(h,e^{\pi i}\alpha_1)$, the result obtained when the sign of α_1 is changed in the right-hand side of (38). We have

$$L(h,e^{\pi i}\alpha_1) = \frac{H_1^{(1)}(\alpha_2 b)J_1(e^{\pi i}\alpha_1 a)e^{ihz}}{e^{\pi i}\alpha_1 k_2^2 H_1^{(1)}(\alpha_2 a)J_0(e^{\pi i}\alpha_1 a) - \alpha_2 k_1^2 H_0^{(1)}(\alpha_2 a)J_1(e^{\pi i}\alpha_1 a)} . \tag{39}$$

With the application of[8]

$$J_n(e^{\pi i}z) = e^{n\pi i}J_n(z) , \tag{40}$$

(39) becomes

$$L(h,e^{\pi i}\alpha_1) = \frac{e^{\pi i}H_1^{(1)}(\alpha_2 b)J_1(\alpha_1 a)}{e^{\pi i}\alpha_1 k_2^2 H_1^{(1)}(\alpha_2 a)J_0(\alpha_1 a) - e^{\pi i}\alpha_2 k_1^2 H_0^{(1)}(\alpha_2 a)J_1(\alpha_1 a)}$$

$$= L(h,\alpha_1). \tag{41}$$

Hence, L(h) has the same value on both Riemann sheets of α_1. This means that the point $h=k_1$ is not a branch point of the integrand.

3.2 POLES

The integrand has poles where the denominator

$$D(h) \equiv \alpha_1 k_2^2 H_1^{(1)}(\alpha_2 a)J_0(\alpha_1 a) - \alpha_2 k_1^2 H_0^{(1)}(\alpha_2 a)J_1(\alpha_1 a) \tag{42}$$

is zero. The equation

$$D(h) = 0 \tag{43}$$

is a complicated transcendental equation that can not be solved analytically.

For the case of interest, however, it is easy to obtain a rough idea of the locations of the poles in the complex h plane. Since the conductivity of the wire is much greater than that of the outer material, we have $|k_1| >> |k_2|$. This means that, in order to have the second term in (42) be as small in magnitude as the first term, h must be near a zero of $\alpha_2 H_0^{(1)}(\alpha_2 a) J_1(\alpha_1 a)$. Since our branch of $H_0^{(1)}(\alpha_2 a)$ does not have any zeros*, the poles must be located near $h=k_2$ (the zero of α_2) and/or the zeros of $J_1(\alpha_1 a)$. Since the zeros of $J_1(Z)$ are all real, all poles that are not near $h=k_2$, must lie near the α_1 branch cut (where $\alpha_1''=0$) shown as the dashed curves terminating at $\pm k_1$ in Figure 2. In the limit as k_1 tends to infinity, the poles near k_2 tend to k_2 whereas the others tend to infinity.

For very large $|h|$, k_1^2 can be neglected compared to h^2 in the expression (12) for α_1 leading to

$$\alpha_1 \tilde{=} ih \text{ for } h'>0 , \tag{44a}$$

$$\alpha_1 \tilde{=} -ih \text{ for } h'<0 . \tag{44b}$$

In this region, the large-argument approximation

$$J_1(Z) \tilde{=} \sqrt{\frac{2}{\pi Z}} \cos\left(Z - \frac{3\pi}{4}\right) = \sqrt{\frac{2}{\pi Z}} \sin\left(Z - \frac{\pi}{4}\right) \tag{45}$$

can be applied to obtain the locations of the zeros of $J_1(\alpha_1 a)$. This shows that any poles present in this region, must be located near the points

$$h'' = \pm \left(N + \frac{1}{4}\right) \frac{\pi}{a} \tag{46}$$

on the imaginary axis for large integral N.

---

* See Figure 9.4 of Reference 8. The zero shown in the third quadrant is on a different Riemann sheet when our branch cut is used. Numerical calculations have shown that no zeros exist in that quadrant for our branch.

3.3 COMPLETION OF THE CONTOUR

For positive z, we consider the integral

$$P_c(z) = \int_c L(h)dh \qquad (47)$$

with the same integrand as the integral P(z) defined in (37) but evaluated over the closed contour c shown in Figure 2. The contour passes from h'=-R to h'=R along the real axis and then along a circular arc of radius R into the upper half plane until it reaches the α_2 branch cut. It then passes down along the branch cut, around the branch point at k_2, and back up to the same height on the branch cut as where it started. It then continues towards the left along a straight horizontal line until h' reaches $-k_2'$. From there, it follows a circular arc of radius R until it returns to the real axis. As R tends to infinity, the real axis portion of $P_c(z)$ becomes equal to our original integral P(z).

We begin by examining the value of the integral over the portion of c that is off of the real axis. On that portion of c, $|h| \to \infty$ as $R \to \infty$. Hence, we can neglect k_1^2 and k_2^2 compared to h^2 in the definitions of α_1 and α_2 so that α_1 satisfies (44) and $\alpha_2 \tilde{=} -ih$ to the left of the branch cut and $\alpha_2 \tilde{=} ih$ to the right of the branch cut. Since it was shown in Section 2.1 that the value of L(h) is unaffected by a change is sign of α_1, we take $\alpha_1 \tilde{=} ih$ for both positive and negative h'. For large $|h|$, we can use the large argument approximations[8],

$$J_0(Z) \tilde{=} \sqrt{\frac{2}{\pi Z}} \cos\left(Z - \frac{\pi}{4}\right) , \qquad (48a)$$

$$J_1(Z) \tilde{=} \sqrt{\frac{2}{\pi Z}} \sin\left(Z - \frac{\pi}{4}\right) , \tag{48b}$$

$$H_0^{(1)}(Z) \tilde{=} \sqrt{\frac{2}{\pi Z}}\, e^{i\left(Z - \frac{\pi}{4}\right)} , \tag{48c}$$

$$H_1^{(1)}(Z) \tilde{=} -i \sqrt{\frac{2}{\pi Z}}\, e^{i\left(Z - \frac{\pi}{4}\right)}, \tag{48d}$$

valid for large $|Z|$ to approximate the functions in the integrand given in (38). The result is

$$L(h) = \frac{a}{bh}\, e^{\mp h(b-a)+ihz} K(h), \tag{49}$$

where

$$K(h) = \frac{\sin\left(iha - \frac{\pi}{4}\right)}{\mp k_1^2 \sin\left(iha - \frac{\pi}{4}\right) - ik_2^2 \cos\left(iha - \frac{\pi}{4}\right)} \tag{50}$$

with the top sign applying to the right of the vertical branch cut and the lower sign applying to the left.

The factor K(h) is infinite at the locations of the poles which are near points on the imaginary axis with h" given by (46). In order to make sure that c does not pass through a pole, we choose R to given by

$$R = \left(2N + \frac{3}{4}\right) \frac{\pi}{a} \tag{51}$$

for large integral N. We then let $R \to \infty$ in discrete steps by letting $N \to \infty$.

Now, consider the portion of the contour that passes from $h' = k_2$ to $h' = -k_2'$ along a horizontal straight line. For large enough N, h" is approximately equal to R on this line. Hence,

$$h' \tilde{=} \left(2N + \frac{3}{4}\right) \frac{\pi}{a} \tag{52}$$

on the contour. Since the poles are near points that satisfy (46), the value of K(h) is finite along the contour. Moreover, since the functions in K(h) are periodic functions of h" with period of 2π for fixed h', K(h) is independent of N. Hence, from (49), we have

$$\left|L(h)\right| \leq \frac{M}{|h|} e^{-h''z} \quad , \tag{53}$$

where M is the maximum value of $\frac{a}{b} \left|K(h)\right| e^{h'(b-a)}$ along the contour. Hence, the value of the integral along this part of the contour tends to zero exponentially as $N \to \infty$ for positive z.

Next, consider the curved portion of the contour. Here, we have $|h'| \to \infty$ as $R \to \infty$. Hence

$$\cos(iha - \pi/4) = \frac{1}{2}\left(e^{-ha-i\pi/4} + e^{ha+i\pi/4}\right) \tilde{=} \frac{1}{2} e^{\pm(ha+i\pi/4)} \quad , \tag{54a}$$

$$\sin(iha - \pi/4) = \frac{1}{2i}\left(e^{-ha-i\pi/4} - e^{ha+i\pi/4}\right) \tilde{=} \mp \frac{1}{2i} e^{\pm(ha+i\pi/4)}, \tag{54b}$$

for large R where the top sign is used for the right-hand part of the contour and lower sign is used for the left-hand part. Hence,

$$K(h) \tilde{=} \mp \frac{1}{k_1^2+k_2^2} \tag{55}$$

for large R. Combination of (55) and (49) yields

$$L(h) \tilde{=} \mp \frac{a}{bh(k_1^2+k_2^2)} \exp[(-|h'| \mp ih")(b-a)]e^{ihz} \tag{56}$$

for large R. Since $b-a \geq 0$, this is of the form

$$L(h) \tilde{=} f(h)e^{ihz} \tag{57}$$

where $|f(h)| \to 0$ as $|h| \to \infty$. Hence, it follows from the usual proof[12] of Jordan's lemma, that for positive z, the integral over this part of the contour tends to zero as $R \to \infty$.

Since the integral along the portion of c that tends to infinity in the upper half plane has been shown to tend to zero as $R \to \infty$, the only portions that are left to contribute are the real axis and the branch cut. We have

$$P_c(z) = P(z)+B(z) \ , \tag{58}$$

where P(z) is the integral of interest given in (37) and B(z) is the integral around the branch cut. According to Cauchy's theorem of the residues[12]

$$P_c(z)=2\pi i \sum_j R_j(z) \tag{59}$$

where $R_j(z)$ is the residue of the j^{th} pole and the sum is over all of the poles in the upper-half plane on the top Riemann sheet of α_2. Hence, the integral of interest has been transformed to the form

$$P(z) = 2\pi i \sum_j R_j(z) - B(z) \tag{60}$$

for positive z. It remains to evaluate the two terms on the right-hand side of (60) and to interpret them physically.

3.4 COMPLEX MODES

The integrand in $P_c(z)$ can be written in the form

$$L(h) = \frac{H_1^{(1)}(\alpha_2 b) J_1(\alpha_1 a) e^{ihz}}{D(h)} \tag{61}$$

with D(h) defined by (42). Since the poles h_j occur at the zeros of D(h) so that

$$D(h_j) = 0 \ , \tag{62}$$

the residue of the j^{th} pole is given by[13]

$$R_j(z) = \left[\frac{H_1^{(1)}(\alpha_2 b) J_1(\alpha_1 a) e^{ihz}}{\dot{D}(h)}\right]_{h=h_j} \ . \tag{63}$$

Since its z dependence is of the form $e^{ih_j z}$, we see that $R_j(z)$ represents a wave field with axial wave number h_j.

Comparison of (62) with Equation (16) of Section 9.15 of Reference 7 shows that (62) is the equation for the wavenumbers of the complex transverse-magnetic (TM) modes of the wire. Hence, $R_j(z)$ is the contribution of the j^{th} complex TM mode and the first term on the right-hand side of (60) is the sum of the contribution of all complex TM modes with wavenumbers in the upper half plane on the top Riemann sheet of α_2.

To obtain the amplitude of each mode, we need to evaluate $\dot{D}(h)$. By differentiating (42) using

$$\frac{d\alpha}{dh} = -\frac{1}{2}\frac{2h}{(k^2 - h^2)^{1/2}} = -\frac{h}{\alpha} \quad , \tag{64}$$

we find

$$\dot{D}(h) = -h\left[\frac{k_2^2}{\alpha_1} H_1^{(1)}(\alpha_2 a) J_0(\alpha_1 a) + \frac{\alpha_1 a k_2^2}{\alpha_2} \dot{H}_1^{(1)}(\alpha_2 a) J_0(\alpha_1 a)\right.$$

$$+ k_2^2 a H_1^{(1)}(\alpha_2 a) \dot{J}_0(\alpha_1 a) - \frac{k_1^2}{\alpha_2} H_0^{(1)}(\alpha_2 a) J_1(\alpha_1 a)$$

$$\left. - k_1^2 a \dot{H}_0^{(1)}(\alpha_2 a) J_1(\alpha_1 a) - \frac{\alpha_2 k_1^2 a}{\alpha_1} H_0^{(1)}(\alpha_2 a) \dot{J}_1(\alpha_1 a)\right] . \tag{65}$$

The derivatives of the Bessel and Hankel functions are given by the recursion formulas (15) and[8]

$$\dot{J}_1(Z) = J_0(Z) - \frac{J_1(Z)}{Z} \quad , \tag{66a}$$

$$\dot{H}_1^{(1)}(Z) = H_0^{(1)}(Z) - \frac{H_1^{(1)}(Z)}{Z} \quad . \tag{66b}$$

Hence, (65) becomes

$$\dot{D}(h) = -h\left[\frac{k_2^2}{\alpha_1} H_1^{(1)}(\alpha_2 a) J_0(\alpha_1 a) + \frac{\alpha_1 a k_2^2}{\alpha_2}\left[H_0^{(1)}(\alpha_2 a) - \frac{H_1^{(1)}(\alpha_2 a)}{\alpha_2 a}\right] J_0(\alpha_1 a)\right.$$

$$-k_2^2 a H_1^{(1)}(\alpha_2 a) J_1(\alpha_1 a) - \frac{k_1^2}{\alpha_2} H_0^{(1)}(\alpha_2 a) J_1(\alpha_1 a) +$$

$$\left. +k_1^2 a H_1^{(1)}(\alpha_2 a) J_1(\alpha_1 a) - \frac{\alpha_2 k_1^2 a}{\alpha_1} H_0^{(1)}(\alpha_2 a)\left[J_0(\alpha_1 a) - \frac{J_1(\alpha_1 a)}{\alpha_1 a}\right]\right] . \quad (67)$$

Combination of terms and application of

$$\alpha_2^2 - \alpha_1^2 = k_2^2 - k_1^2 \quad , \quad (68a)$$

$$\alpha_1^2 k_2^2 - \alpha_2^2 k_1^2 = h^2(k_1^2 - k_2^2) \quad , \quad (68b)$$

yields

$$\dot{D}(h) = h(k_1^2 - k_2^2)\left[\frac{k_2^2}{\alpha_1 \alpha_2^2} H_1^{(1)}(\alpha_2 a) J_0(\alpha_1 a) - \frac{ah^2}{\alpha_1 \alpha_2} H_0^{(1)}(\alpha_2 a) J_0(\alpha_1 a)\right.$$

$$\left. -a H_1^{(1)}(\alpha_2 a) J_1(\alpha_1 a) + \frac{k_1^2}{\alpha_1 \alpha_2^2} H_0^{(1)}(\alpha_2 a) J_1(\alpha_1 a)\right] . \quad (69)$$

It follows from the equation (43) for locations of the poles that the first and last terms in the square bracket in (69) are equal when $\dot{D}(h)$ is evaluated at a pole h_j. Hence,

$$\dot{D}(h_j) = \frac{h_j(k_1^2-k_2^2)}{\alpha_1^2\alpha_2}\left[2k_1^2H_0^{(1)}(\alpha_2 a)J_1(\alpha_1 a) - ah_j^2\alpha_1 H_0^{(1)}(\alpha_2 a)J_0(\alpha_1 a)\right.$$

$$\left.-a\alpha_1^2\alpha_2 H_1^{(1)}(\alpha_2 a)J_1(\alpha_1 a)\right] . \qquad (70)$$

where h in α_1 and α_2 is to be evaluated at h_j. Equation (70) is the final exact expression for $\dot{D}(h_j)$ to be substituted into the expression (63) for the residue of the pole h_j.

The properties of the modes of a wire in air have been studied by Sommerfeld (see Reference 14 for an account of Sommerfeld's results). He found that there is one mode with wave number h_0 near k_2 on the upper Riemann sheet. He called this mode the principal mode and the others he called secondary modes. *The secondary modes are attenuated much more* than the principal one. In fact, since the wavenumber of the secondary modes lie near the dashed line in Figure 2 that goes above k_1 in the complex plane, $h_j'' > k_1''$ for all of these modes. Hence, they are attenuated even faster than is a plane wave propagating in the metal. This shows that the secondary modes are damped immediately and can be neglected after a very short distance along the wire. For this reason, we now concentrate on the principal mode, which we label by $j=0$.

Since $h_0 \tilde{=} k_2$ and since $|k_1| >> |k_2|$, the second term in the square brackets in (70) is negligible compared to the first term. Hence, the expression (63) for the residue of the pole becomes

$$R_0(z) \tilde{=} \frac{\alpha_1^2\alpha_2 H_1^{(1)}(\alpha_2 b)e^{ih_0 z}}{h_0(k_1^2-k_2^2)[2k_1^2H_0^{(1)}(\alpha_2 a)-a\alpha_1^2\alpha_2 H_1^{(1)}(\alpha_2 a)]} , \qquad (71)$$

where h in α_1 and α_2 is to be evaluated at h_0. Next, we apply the approximations $k_1^2 - k_2^2 \tilde{=} k_1^2$ and $\alpha_1 \tilde{=} k_1$ to obtain

$$R_0(z) \tilde{=} \frac{\alpha_2 H_1^{(1)}(\alpha_2 b) e^{ih_0 z}}{h_0 k_1^2 [2H_0^{(1)}(\alpha_2 a) - a\alpha_2 H_1^{(1)}(\alpha_2 a)]} . \qquad (72)$$

Finally, since $|\alpha_2 b|$ is very small for the principal mode, we apply the small-argument approximations of the Hankel functions*

$$H_0^{(1)}(Z) = \frac{2i}{\pi} \ln\left(\frac{\Gamma Z}{2i}\right) , \qquad (73a)$$

$$H_1^{(1)}(Z) = -\frac{2i}{\pi Z} , \qquad (73b)$$

valid for small $|Z|$ where $\Gamma = e^{\gamma}$ and $\gamma = 0.577216$ is Euler's constant. The result is

$$R_0(z) \tilde{=} -\frac{e^{ih_0 z}}{bh_0 k_1^2 \left[2\ln\left(\frac{\Gamma\alpha_2 a}{2i}\right) + 1\right]} . \qquad (74)$$

where α_2 is to be evaluated at $h = h_0$.

---

* Reference 8, page 360. The factor 1/i in the argument of the logarithm in (73a) accounts for the contribution of $J_0(z) \tilde{=} 1$ for small $|z|$. We apply the principal branch of ln(z) which has branch cut lying along the negative real axis. With this choice, the right-hand side of (73a) has the same branch cut as the left-hand side.

According to (60), the contribution of $R_0(z)$ to the integral $P(z)$ is $2\pi i R_0(z)$. Hence, it follows from (36) that the contribution $I_p(z)$ of the principal mode to the current in the wire is

$$I_p = - V_0 k_2^2 \sigma_1 b 2\pi i R_0(z) \tag{75}$$

Application of our approximate expression (74) for the residue $R_0(z)$ therefore gives

$$I_p = \frac{2\pi i V_0 k_2^2 \sigma_1 e^{ih_0 z}}{h_0 k_1^2 [2 \ln (\frac{\Gamma \alpha_2 a}{2i}) + 1]} \quad . \tag{76}$$

Since $\sigma_1 / k_1^2 \to (i\mu\omega)^{-1}$ as $\sigma_1 \to \infty$ [see (3) and (4)], we see that $I_p \to 0$ as $\sigma_1 \to \infty$. This means that the principal mode is not excited by the generator if the wire is perfectly conducting.* It should be noted, however, that I_p tends to zero rather slowly as σ_1 tends to infinity because $\ln(\alpha_2 a)$ tends to infinity slowly. This means that the contribution of the principal mode to the current might be significant even with highly conducting wires. To answer the question definitively, it is necessary to solve for h_0 numerically in order to obtain an accurate value of α_2.

Another important question that must be answered numerically is whether the wavenumber h_0 lies on the upper or lower Riemann sheet. For the case treated by Sommerfeld (see Reference 14), it is known that h_0 lies on the upper sheet. As the parameters vary, however, h_0 can cross the branch cut to the lower sheet. In that case, the residue of the pole does not contribute to the current.

---

* It can be shown easily that the same is true for all of the other modes as well. This is the reason that modes do not appear in the analysis in Reference 3.

3.5 SPACE WAVE

In order to obtain a physical interpretation of the branch cut integral B(z), we examine its asymptotic behavior for large z. Since the imaginary part of h increases as we move up either side of the branch cut from the branch point k_2, the integrand L(z) decreases exponentially. Hence, for large enough z, only the vicinity of the branch point contributes to the integral. Near the branch point, it is useful to write D(h) in the form

$$D(h) = \alpha_1 k_2^2 H_1^{(1)}(\alpha_2 a) J_0(\alpha_1 a) \left[1 - \frac{\alpha_2 k_1^2 H_0^{(1)}(\alpha_2 a) J_1(\alpha_1 a)}{\alpha_1 k_2^2 H_1^{(1)}(\alpha_2 a) J_0(\alpha_1 a)}\right]. \quad (77)$$

Since $\alpha_2=0$ at the branch point, the second term in the bracket is much smaller than 1. Hence, we can expand $D^{-1}(h)$ in the form

$$\frac{1}{D(h)} \tilde{=} \left[\alpha_1 k_2^2 H_1^{(1)}(\alpha_2 a) J_0(\alpha_1 a)\right]^{-1} \left[1 + \frac{\alpha_2 k_1^2 H_0^{(1)}(\alpha_2 a) J_1(\alpha_1 a)}{\alpha_1 k_2^2 H_1^{(1)}(\alpha_2 a) J_0(\alpha_1 a)} + \ldots\right]. \quad (78)$$

Neglecting the higher order terms and substituting into the definition (38) of the integrand L(h), we find

$$L(h) \tilde{=} \frac{H_1^{(1)}(\alpha_2 b) J_1(\alpha_1 a)}{\alpha_1 k_2^2 H_1^{(1)}(\alpha_2 a) J_0(\alpha_1 a)} \left[1 + \frac{\alpha_2 k_1^2 H_0^{(1)}(\alpha_2 a) J_1(\alpha_1 a)}{\alpha_1 k_2^2 H_1^{(1)}(\alpha_2 a) J_0(\alpha_1 a)}\right] e^{ihz} . \quad (79)$$

Since $|\alpha_2| b$ and $|\alpha_2| a$ are small near the branch point, we apply the small-argument approximations (73) for the Hankel functions in (79).

The result is

$$L(h) \tilde{=} \frac{aJ_1(\alpha_1 a)}{b\alpha_1 k_2^2 J_0(\alpha_1 a)} \left[1 - \frac{ak_1^2\alpha_2^2 J_1(\alpha_1 a)}{k_2^2\alpha_1 J_0(\alpha_1 a)} \ln\left(\frac{\Gamma\alpha_2 a}{2i}\right)\right] e^{ihz} . \qquad (80)$$

We next determine the discontinuity of L(h) across the branch cut which results from a change in sign of α_2. We have

$$\alpha_2 = \sqrt{k_2^2 - h^2} = \sqrt{k_2 + h}\sqrt{k_2 - h} . \qquad (81)$$

The first square root in (81) is the same on opposite sides of the branch cut because $k_2 + h$ does not change as h encircles the branch point. The second square root, however, is different. The argument of $k_2 - h$ is $-\pi/2$ on the left side and $3\pi/2$ on the right. Hence, the argument of $\sqrt{k_2 - h}$ is $-\pi/4$ on the left and $3\pi/4$ on the right. Since $\ln z = \ln|z| + i(\text{argument of } z)$ with $-\pi < (\text{argument of } z) < \pi$, the discontinuity of the logarithm in (80) can be written

$$\ln\left(\frac{\Gamma\alpha_2 a}{2i}\right)\Bigg|_{\text{left side}} - \ln\left(\frac{\Gamma\alpha_2 a}{2i}\right)\Bigg|_{\text{right side}} = -\pi i . \qquad (82)$$

The corresponding discontinuity in L(h) from left side to right side is therefore

$$\frac{\pi i}{b}\left[\frac{ak_1 J_1(\alpha_1 a)\alpha_2}{k_2^2 J_0(\alpha_1 a)\alpha_1}\right]^2 e^{ihz} . \qquad (83)$$

As a result, the branch cut integral is

$$B(z) \tilde{=} \frac{\pi i}{b}\left[\frac{ak_1 J_1(\hat{\alpha}_1 a)}{k_2^2 J_0(\hat{\alpha}_1 a)\hat{\alpha}_1}\right]^2 B_0 , \qquad (84)$$

where

$$\hat{\alpha}_1 = \sqrt{k_1^2 - k_2^2} \ , \tag{85}$$

$$B_0 = \int_{k_2}^{k_2+i\infty} \alpha_2^2 \, e^{ihz} \, dh \ . \tag{86}$$

The integral B_0 can be evaluated exactly. Let

$$h = k_2 + i\kappa \ . \tag{87}$$

Then B_0 becomes

$$B_0 = \int_0^\infty [k_2^2 - (k_2^2 + 2i\kappa k_2 - \kappa^2)] \, e^{ik_2 z} \, e^{-\kappa z} i \, d\kappa$$

$$= ie^{ik_2 z}\left(\frac{\partial^2}{\partial z^2} + 2ik_2\frac{\partial}{\partial z}\right) \int_0^\infty e^{-\kappa z} d\kappa$$

$$= ie^{ik_2 z}\left(\frac{\partial^2}{\partial z^2} + 2ik_2\frac{\partial}{\partial z}\right) \frac{1}{z}$$

$$= \frac{2i}{z^3} \, e^{ik_2 z}(1 - ik_2 z) \ . \tag{88}$$

Substitution of (88) into (84) gives the asymptotic expression

$$B(z) = \frac{-2\pi}{b} \left[\frac{ak_1 J_1(\hat{\alpha}_1 a)}{k_2^2 J_0(\hat{\alpha}_1 a)\hat{\alpha}_1}\right]^2 \frac{1 - ik_2 z}{z^3} \, e^{ik_2 z} \tag{89}$$

valid for large z.

For high frequency applications, the factor in the brackets in (89) can be simplified by using the approximation $\hat{a}_1 \tilde{=} k_1$ and noting that $|k_1|a \gg 1$ for typical wires.[14] Hence, we can use the large-argument approximations (48a-b) of the Bessel functions. Since $k_1 a$ has large positive imaginary part, (48a-b) can be written

$$J_0(\hat{\alpha}_1 a) \tilde{=} \frac{1}{\sqrt{2\pi k_1 a}} e^{-i(k_1 a - \pi/4)} , \tag{90a}$$

$$J_1(\hat{\alpha}_1 a) \tilde{=} \frac{i}{\sqrt{2\pi k_1 a}} e^{-i(k_1 a - \pi/4)} . \tag{90b}$$

Consequently, we have

$$\frac{J_1(\hat{\alpha}_1 a)}{J_0(\hat{\alpha}_1 a)} \tilde{=} i \tag{91}$$

The approximate expression for B(z) then becomes

$$B(z) \tilde{=} \frac{2\pi a^2}{b} \frac{1-ik_2 z}{k_2^4 z^3} e^{ik_2 z} \tag{92}$$

for large z and high frequency.

The contribution $I_B(z)$ of the branch-cut integral to the current in the wire is found by combining (89), (60) and (36) to obtain

$$I_B(z) \tilde{=} -\frac{2\pi V_0 \sigma_1}{k_2^2} \left[\frac{a k_1 J_1(\hat{\alpha}_1 a)}{\hat{\alpha}_1 J_0(\hat{\alpha}_1 a)}\right]^2 \frac{1-ik_2 z}{z^3} e^{ik_2 z} \tag{93}$$

for large z.

The quantity B_0 given in (88) is proportional to the z component of the electric field radiated by a point electric dipole[15] located at the origin in a homogeneous medium with wavenumber k_2. We are led, therefore, to the following physical interpretation. The branch-cut integral yields a current driven by the component along the wire of the electric field of an electromagnetic wave that is radiated out by the generator. Far from the generator, this wave has the same spatial dependence as it would have if it were being radiated in the outer material without the wire present. The primary* effect of the wire is to weakly influence the magnitude of the wave through the multiplicative factor in (84). Note that this is true even inside the wire, where the wavenumber is very different from k_2. Because of these properties, the electromagnetic field corresponding to the branch-cut integral is frequently called a "space wave."[11] It is a field that is radiated into space rather than being guided by the wire (as are the modes). The geometrical factor $(1-ik_2z)/z^3$ occurring in (93) is due to the "radiation spreading" of the wave. The reason this fall off is faster than the 1/z behavior of a radiation field is that the current is produced by the z component of the electric field which is the radial component. The radiation field that falls off as 1/z is the transverse electromagnetic field which does not generate currents along the wire.

Although the approximate expression (92) for B(z) is independent of wire conductivity, the range of validity of (92) is highly dependent on σ_1. This is evident from the derivation of the result. In order for us to be able to apply the expansion used in (78), it is necessary for the second term in the square brackets in (77) to be much smaller than one in magnitude over the portion of the branch cut where the integrand is not negligible. But the magnitude of the second term grows rapidly with increasing distance from the branch point because $|k_1|^2/|k_2|^2$ is large.

---

* There is another "effect" of the wire discussed in the next paragraph.

Hence, z must be large enough so that the factor e^{ihz} causes the integrand to be negligible all along the cut except very near the branch point. The larger is the conductivity of the wire, the faster the second term in (77) grows and therefore the larger z must be in order for the result (92) to be valid.

We now obtain a rough estimate of the range of validity of (92). The second term in (77) is nearly equal to 1 at the locations of poles. The pole h_0 is located very near and slightly above the branch point.* Hence, the second term in (77) becomes comparable to 1 when the point of integration on the branch cut reaches the height h_0'' of the pole. Therefore, in order for our expansion of (77) in the form of (78) to be valid, the factor $e^{-h_0''z}$ must be negligible compared to $e^{-k_2''z}$. The first quantity will be down by a factor e^{-1} compared to the second if $(-h_0''+k_2'')z = -1$. Hence, the asymptotic result is valid if z is much larger than the distance

$$z_c = \frac{1}{h_0''-k_2''} . \qquad (94)$$

This distance can be very large because h_0 can be very close to k_2. Since h_0 approaches k_2 as the wire conductivity increases, the asymptotic result is valid only at very large distances for a highly conducting wire. As $\sigma_1 \to \infty$, the result is not valid anywhere.**

It is helpful to consider a specific example. Sommerfeld has shown[14] that

---

* This is known from previous numerical studies of the principal mode. See Reference 14.

** In this limit, the results of Reference 3 and 4 are valid.

$$h_0 \tilde{=} k_2[1+(6.0+6.4i)10^{-5}] \qquad (95)$$

for the case of a 1mm radius copper wire in air with frequency of 10^9 Hz. Since $k_2'' = 0$ for air, (94) and (95) together require that

$$k_2' z_c = 1.6\times10^4 \ .$$

Hence, z must be much more than 2.5×10^3 wavelengths in air or about 720m for (92) to be valid in this case. Other numerical examples are presented in Section 3.

3.6 NEAR ZONE

Since z must be so large for the asymptotic result to be valid, we obtain in this section a rough idea of the behavior of the current much closer to the source. We wait until later to specify how small z must be for the approximations to be valid, but it can be stated at this point that z must be much less than z_c. On the other hand we require that z be large enough so that the small-argument approximations can be used for the Hankel functions over the portion of the branch cut where the integrand is not negligible.

On the branch cut, we have $h=k_2+i\kappa$ with $\kappa\geq0$ according to (87). Since

$$\alpha_2^2 \equiv (k_2+h)(k_2-h) \tilde{=} -2ik_2\kappa \tag{96}$$

for small κ, we see that the arguments of the Hankel functions are small if $\kappa << (2|k_2|b^2)^{-1}$. We want the integrand to be negligible for κ outside this range. To that end, we require that $z >> z_d$ where z_d is defined by

$$z_d = 2|k_2|b^2 . \tag{97}$$

Then, the integrand is negligible for κ too large for the small argument approximations to be used because

$$\left| e^{i(k_2+i\kappa)z_d} / e^{ik_2 z_d} \right| < e^{-1} \tag{98}$$

for $k \geq (2|k_2|b^2)^{-1}$. Hence, the region of interest satisfies

$$z_d << z << z_c \tag{99}$$

with z_d and z_c defined by (97) and (94) respectively. Since

$$\frac{1}{h_0''-k_2''} >> 2b^2|k_2| \tag{100}$$

for highly conducting wires with small diameters and with the source near the wire, (99) covers a wide range of distances.

We now employ the small-argument approximations (73) for the Hankel functions in the expression (38) for the integrand

$$L(h) \tilde{=} \frac{aJ_1(\alpha_1 a)e^{ihz}}{b\alpha_1 k_2^2 J_0(\alpha_1 a) + ab\alpha_2^2 k_1^2 J_1(\alpha_1 a) \ln\left(\frac{\Gamma \alpha_2 a}{2i}\right)} . \tag{101}$$

This expression can be simplified further by noting that when h is near k_2, $\alpha_1 \tilde{=} k_1$ for $|k_1| >> |k_2|$. Then (101) becomes

$$L(h) \tilde{=} \frac{aJ_1(k_1a)e^{ihz}}{bk_1[k_2^2 J_1(k_1a)+ak_1\alpha_2^2 J_1(k_1a)\ln(\frac{\Gamma\alpha_2 a}{2i})]} . \qquad (102)$$

The discontinuity in the logarithm in (102) across the branch cut has already been discussed and is presented in (82). It follows from that discussion that the argument of $[(k_2-h)/i]^{1/2}$ is given by

$$\arg\sqrt{i(h-k_2)} = \pm\frac{\pi}{2} \qquad (103)$$

on the branch cut where the top sign applies to the right side and the bottom sign applies to the left. Hence, the logarithm can be written

$$\ln(\frac{\Gamma\alpha_2 a}{2i}) = \ln(\frac{\Gamma a\sqrt{-i(k_2+h)}}{2}) + \ln(\sqrt{i(h-k_2)}$$

$$\tilde{=} \ln(\frac{\Gamma a\sqrt{-2k_2}}{2}) + \ln\sqrt{\kappa} \pm \frac{\pi}{2} i$$

$$= \ln(\frac{\Gamma a}{2}\sqrt{-i2k_2\kappa}) \pm \frac{\pi}{2} i \quad , \qquad (104)$$

where the approximation $k_2+h \tilde{=} 2k_2$ has been used. To eliminate the square root in (104), it is convenient to write

$$\ln(\frac{\Gamma\alpha_2 a}{2i}) \tilde{=} \frac{1}{2}[\ln(A\kappa)) \pm \pi i] , \qquad (105)$$

where

$$A = \frac{\Gamma^2 a^2 k_2}{2i} \quad . \tag{106}$$

Substitution of (96) and (105) into (102) yields

$$L_{\pm}(h) \tilde{=} \frac{aJ_1(k_1 a)e^{ihz}}{bk_1 k_2\{k_2 J_0(k_1 a) - i\kappa a k_1 J_1(k_1 a)[\ln(A\kappa) \pm \pi i]\}} \quad , \tag{107}$$

where $L_+(h)$ is the integrand on the right side of the branch cut and $L_-(h)$ is the integrand on the left side of the branch cut.

Since the contour of the branch-cut integral passes down the right side and up the left side of the branch cut, the integral can be written

$$B(z) = i \int_0^{\infty} [L_-(h) - L_+(h)]d\kappa \tag{108}$$

with $h = k_2 + i\kappa$. If we introduce the constant

$$W = i \frac{J_0(k_1 a)}{J_1(k_1 a)} \quad , \tag{109}$$

the integrand in (108) becomes

$$L_-(h) - L_+(h) = \frac{a}{bk_1 k_2} \frac{2ak_1 \kappa \pi e^{ihz}}{[-iWk_2 - iak_1 \kappa \ln(A\kappa)]^2 - (ak_1 \pi \kappa)^2} \quad . \tag{110}$$

Hence, the branch-cut integral is

$$B(z) = -\frac{2\pi i a^2}{bk_2} e^{ik_2 z} \int_0^\infty \frac{\kappa e^{-\kappa z} d\kappa}{\left[Wk_2 + ak_1 \kappa \ln(A\kappa)\right]^2 + (ak_1 \pi \kappa)^2} . \quad (111)$$

We note that for high-frequency applications when the large-argument approximations can be used for the Bessel functions, then W reduces to 1 according to (91). Otherwise, W is a constant that depends on the frequency and the properties of the wire.

For κ very near zero, the denominator in (111) is dominated by the first term Wk_2 in the square brackets. The second term grows very rapidly with increasing κ, however, because $|k_1| >> |k_2|$, and eventually it dominates over the first. Let κ_m be the smallest value of κ such that Wk_2 can be neglected in (111) for $\kappa \geq \kappa_m$. Then $B(z)$ can be approximated by

$$B(z) = B_m(z) + B_p(z) \quad (112)$$

where

$$B_m(z) = -\frac{2\pi i a^2}{bk_2} e^{ik_2 z} \int_0^{\kappa_m} \frac{\kappa e^{-\kappa z} d\kappa}{\left[Wk_2 + ak_1 \kappa \ln(A\kappa)\right]^2 + (ak_1 \kappa \pi)^2} , \quad (113)$$

$$B_p(z) = -\frac{2\pi i}{bk_1^2 k_2} e^{ik_2 z} \int_{\kappa_m}^\infty \frac{e^{-\kappa z} d\kappa}{\kappa\left[\ln^2(A\kappa) + \pi^2\right]} . \quad (114)$$

It is difficult to learn much about $B_m(z)$ without employing numerical techniques. Two points can be made, however. First we note that for* $z_d << z << 1/\kappa_m$, the z dependence of $B_m(z)$ arises only from the factor $e^{ik_2 z}$. Hence, $B_m(z)$ does not decrease due to the geometrical spreading of the space wave. Secondly, we note that since $\kappa_m \to 0$ as $\sigma_1 \to \infty$, $B_m(z)$ tends to zero as the wire tends toward a perfect

*Since $\kappa_m > h_0'' - k_2''$, this restriction requires that $z << z_c$.

conductor. This means that $B_m(z)$ may be small compared to $B_p(z)$ for highly conducting wire.

We now turn our attention to $B_p(z)$. The integral in (114) is the same as occurs in the treatment of a perfect conductor in Section 4 of Reference 3 except that (a) our factor A defined* in (106) is complex whereas it is purely imaginary in Reference 3 and (b) the lower limit of our integral is κ_m whereas it is zero in Reference 3. As a result, we can approximate $B_p(z)$ by the procedure used in Reference 3 with minor modifications.

To that end, consider the integral

$$I(z) = \int_{\kappa_m}^{\infty} \frac{e^{-\kappa z} d\kappa}{\kappa[\ln^2(A\kappa)+\pi^2]} \quad . \tag{115}$$

Because of the factor $e^{-\kappa z}$, the integrand is negligible for κ larger than some number α which is small enough that $|\ln(A\kappa)| >> \pi$ for $\kappa << \alpha$. Hence, the term in the square brackets can be expanded in a binomial series to obtain

$$I(z) = \sum_{n=1}^{\infty} I_n \tag{116}$$

where

$$I_n = (-1)^{n+1} \pi^{2n-2} \int_{\kappa_m}^{\infty} \frac{e^{-\kappa z} d\kappa}{\kappa \ln^{2n}(A\kappa)} \quad . \tag{117}$$

---

* Note also that our A is defined differently than the A of Reference 3.

We now change the integration variable to

$$\zeta = -\ln(A\kappa) \tag{118}$$

to obtain

$$I_n = (-1)^{n+1}\pi 2n-2 \int_{c_\zeta} \frac{\exp\left[-\frac{z}{A}e^{-\zeta}\right]}{\zeta^{2n}} d\zeta \tag{119}$$

where c_ζ is a horizontal straight line a distance arg(A) below the real axis in the complex ζ plane starting at $-\infty$-iarg A and ending at $-\ln(A\kappa_m)$.

The exponent $-\frac{z}{A}e^{-\zeta}$ is real and negative all along c_ζ. Hence, the integral over the portion of the contour to the left of

$$\zeta_0 = -\ln(A/z) \tag{120}$$

can be approximated by

$$I_n^{(-)} = (-1)^{n+1}\pi 2n-2 \int_{-\infty-i\arg A}^{\zeta_0} \frac{\exp\left[-\frac{z}{A}e^{-\zeta}\right]}{\zeta_0{}^{2n}} d\zeta \tag{121}$$

because the integrand decays so rapidly as ζ moves away from ζ_0 along c_ζ to the left.

In the integral to the right of ζ_0, the exponential term $\exp[-\frac{z}{A}e^{-\zeta}]$ is approximately equal to one except in the immediate vicinity of ζ_0. Hence, we approximate this integral by

$$I_n^{(+)} = (-1)^{n+1}\pi 2n-2 \int_{\zeta_0}^{-\ln(A\kappa_m)} [\frac{1}{\zeta^{2n}} + \frac{\exp[-\frac{z}{A}e^{-\zeta}]-1}{\zeta_0{}^{2n}}]\, d\zeta$$

$$= (-1)^{n+1}\pi 2n-2\{-\frac{1}{2n-1}[\frac{1}{-\ln(A\kappa_m)}]^{2n-1} + \frac{1}{2n-1}\frac{1}{\zeta_0{}^{2n-1}}$$

$$+ \frac{\ln(A\kappa_m)}{\zeta_0{}^{2n}} + \frac{1}{\zeta_0{}^{2n-1}} + \frac{1}{\zeta_0{}^{2n}} \int_{\zeta_0}^{-\ln(A\kappa_m)} \exp[-\frac{z}{A}e^{-\zeta}]\, d\zeta\}. \quad (122)$$

The total integral is then

$$I_n = I_n^{(-)} + I_n^{(+)} = (-1)^{n+1}\pi 2n-2\{\frac{1}{2n-1}[\frac{1}{\ln(A\kappa_m)}]^{2n-1} + \frac{2n}{(2n-1)\zeta_0{}^{2n-1}} +$$

$$+ \frac{\ln(A\kappa_m)}{\zeta_0{}^{2n}} + \frac{1}{\zeta_0{}^{2n}} \int_{C_\zeta} \exp[-\frac{z}{A}e^{-\zeta}]d\zeta\}\ . \quad (123)$$

By changing the integration variable back to κ, the integral on the right-hand side of (123) becomes

$$\int_{C_\zeta} \exp[-\frac{z}{A}e^{-\zeta}]d\zeta = \int_{\kappa_m}^{\infty} \frac{e^{-\kappa z}}{\kappa}\, d\kappa = E_1(\kappa_m z)\ , \quad (124)$$

where $E_1(\kappa_m z)$ is the exponential integral of order 1. For $z \ll 1/\kappa_m$, we can apply the small argument approximation[16] of $E_1(\kappa_m z)$.

$$E_1(\kappa_m z) \tilde{=} -\ln(\Gamma \kappa_m z). \tag{125}$$

Hence, the integral I_n can approximated by

$$I_n \tilde{=} (-1)^{n+1} \pi^{2n-2} \left\{ \frac{1}{2n-1} \left[\frac{1}{\ln(A\kappa_m)} \right]^{2n-1} - \frac{2n}{2n-1} \left[\frac{1}{\ln(A/z)} \right]^{2n-1} \right.$$

$$\left. + \frac{\ln[A/(\Gamma z)]}{\ln^{2n}(A/z)} \right\} \tag{126}$$

for $z_d \ll z \ll 1/\kappa_m$.

From the definition of A given in (106) and z_d given in (97), we have

$$|A| = \frac{\Gamma^2 a^2}{4b^2} z_d \tag{127}$$

Since $\Gamma^2/4 \tilde{=} 0.8$ and $a<b$, the condition that $z \gg z_d$ guarantees that $|A|/z \ll 1$ and $|\ln(A/z)| > 1$. Hence, it is useful to note that (126) shows that

$$I_n = O\left\{ \left[\frac{1}{\ln(A/z)} \right]^{2n-1} \right\}. \tag{128}$$

for $z < 1/\kappa_m$.

This means that the series expansion of I(z) given in (116) is dominated by I_1. From (126), we have

$$I_1 = \frac{1}{\ln(A\kappa_m)} - \frac{2}{\ln(A/z)} + \frac{\ln[A/(\Gamma z)]}{\ln^2(A/z)} \quad . \tag{129}$$

By combining the last two terms, this can be written

$$I_1 = \frac{1}{\ln(A\kappa_m)} - \frac{1}{\ln(A/z)}\left[1 - \frac{\ln(1/\Gamma)}{\ln(A/z)}\right] \quad . \tag{130}$$

The last term in (130) is observed to be the first part of the binomial expansion

$$\frac{1}{\ln\left(\frac{A}{\Gamma z}\right)} = \frac{1}{\ln(A/z)[1+\ln(1/\Gamma)/\ln(A/z)]} = \frac{1}{\ln(A/z)}\left[1 - \frac{\ln(1/\Gamma)}{\ln(A/z)}\right]$$

$$+ O\left[\frac{1}{\ln^3(A/z)}\right] \quad . \tag{131}$$

Hence, (130) becomes

$$I_1 = \frac{1}{\ln(A\kappa_m)} - \frac{1}{\ln\left(\frac{A}{\Gamma z}\right)} + O\left[\frac{1}{\ln^3(A/z)}\right] \quad . \tag{132}$$

Finally, we combine (116), (128), and (132) to obtain the expression for I(z)

$$I(z) = \frac{1}{\ln(A\kappa_m)} - \frac{1}{\ln\left(\frac{A}{\Gamma z}\right)} + O\left[\frac{1}{\ln^3(A/z)}\right] \tag{133}$$

valid for $z_d << z << 1/\kappa_m$. This result reduces to the result in Section 4 of Reference 3 in the limit as $\sigma_1 \to \infty$ because $\kappa_m \to 0$ in that limit.

With the application of (133) in (114), the portion $B_p(z)$ of the branch-cut integral can be approximated by

$$B_p(z) \simeq \frac{2\pi i}{bk_1^2 k_2} e^{ik_2 z} \left[\frac{1}{\ln\left(\frac{A}{\Gamma z}\right)} - \frac{1}{\ln(A\kappa_m)}\right] . \qquad (134)$$

The total branch-cut integral can then be written

$$B(z) \simeq \frac{2\pi i}{bk_1^2 k_2} e^{ik_2 z} \left[\frac{1}{\ln\left(\frac{A}{\Gamma z}\right)} - Q\right] , \qquad (135)$$

where

$$Q = \frac{1}{\ln(A\kappa_m)} + (k_1 a)^2 \int_0^{\kappa_m} \frac{\kappa e^{-\kappa z} d\kappa}{\left[Wk_2 + ak_1 \kappa \ln(A\kappa)\right]^2 + (ak_1 \kappa \pi)^2} \qquad (136)$$

for $z_d << z << 1/\kappa_m$.

The contribution of the first term in the brackets in (135) is the asymptotic value of the branch-cut integral for a perfect conductor. Hence, the contribution of the second term is the change introduced by the finite conductivity of the wire. It is nearly independent of z for small z and tends to zero in the limit as $\sigma_1 \to \infty$. We determine its value numerically for a case of interest in the next section.

SECTION 4
CURRENT DISTRIBUTION ALONG THE WIRE

In this section, we combine, summarize, and discuss the analytical results obtained in the previous sections and present numerical examples. Throughout the section, the source is taken to be on the wire by setting b equal to a.

4.1 SUMMARY OF ANALYTICAL RESULTS

The current produced by a δ function voltage generator of strength V_0 located on the wire at $z=0$ can be written for positive z in the form

$$I(z) = I_{mode}(z) + I_{space}(z) \tag{137}$$

by combining (36) with (60).

The first term in (137),

$$I_{mode}(z) = -V_0 \, k_2^2 \, \sigma_1 a 2\pi i \sum_j R_j(z) \, , \tag{138}$$

is the contribution of the complex TM modes guided by the wire with wavenumbers h_j that satisfy the modal equation (43). All of these modes except one (known as the principal mode) are damped out immediately away from the generator. The wavenumber h_0 of the principal mode is very close

to k_2 (the wave number of the material surrounding the wire) and it can lie on either Riemann sheet of the square root $\alpha_2 = (k_2^2-h_0^2)^{1/2}$. If h_0 lies on the upper sheet, the principal mode contributes to the current in the wire and the mode is said to have been excited. If h_0 is on the lower sheet, the mode does not contribute to the current (R_0 is then taken to be zero) and the mode is not excited.

When it is excited, the current produced by the principal mode is given to a good approximation for highly conducting wires by (76),

$$I_{mode}(z) \tilde{=} \frac{2\pi i V_0 k_2^2 \sigma_1 e^{ih_0 z}}{h_0 k_1^2 [2\ln(\frac{\Gamma\alpha_2 a}{2i}) + 1]} , \tag{139}$$

where $\alpha_2^2 \tilde{=} 2k_2(k_2-h_0)$. If we set

$$h_0 = k_2+\delta \tag{140}$$

in the expression for α_2 and $h_0 = k_2$ in the denominator of (121), then (139) can be written

$$I_{mode}(z) \tilde{=} \frac{2\pi i V_0 k_2 \sigma_1 e^{ih_0 z}}{k_1^2 [\ln(A\delta)+1]} , \tag{141}$$

where A is given by (106).

In order to evaluate (141) for any specific case, it is necessary to solve the modal equation (43) numerically to determine h_0 (and hence δ). This is necessary also, in order to determine whether or not the mode is excited by determining whether h_0 is on the upper or lower Riemann sheet. It has been found numerically that the imaginary part of

h_0 is always slightly larger than k_2''. This means that the attenuation of the principal mode is slightly greater than that of a plane wave in the surrounding material.

The second term in (137),

$$I_{space}(z) = V_0 k_2^2 \sigma_1 a B(z) \tag{142}$$

is the contribution of an electromagnetic wave (known as a space wave) that radiates from the generator out into the material surrounding the wire. The wave number of this wave is equal to that of the surrounding material but its amplitude decreases with distance from the generator because of the geometrical spreading of the wave as it propagates.

The distribution of current along the wire is given in (142) in terms of the branch-cut integral B(z). If $z \gg z_d = 2|\kappa_2|a^2$ so that the small argument approximations can be used to approximate the Hankel functions in the integrand, B(z) is given by (111) with b=a. The resulting expression for the current is

$$I_{space}(z) \tilde{=} -2\pi i V_0 k_2 \sigma_1 a^2 e^{ik_2 z} \int_0^\infty \frac{\kappa e^{-\kappa z} d\kappa}{[Wk_2 + ak_1 \kappa \ln(A\kappa)]^2 + (ak_1 \pi \kappa)^2}, \tag{143}$$

with W given by (109).

If $z \gg z_c = (h_0'' - k_2'')^{-1}$, then $I_{space}(z)$ can be approximated by (93) (with $\hat{\alpha}_1 \tilde{=} k_1$) as

$$I_{space}(z) \tilde{=} + \frac{2\pi V_0 \sigma_1}{k_2^2} \left[\frac{a}{W}\right]^2 \frac{1 - ik_2 z}{z^3} e^{ik_2 z}. \tag{144}$$

This is the current that would be generated in the far field of an electric dipole located at the origin and radiating into a homogeneous material with wave number k_2. The reason that the current falls off faster than $1/z$ is that it is driven by the longitudinal electric field rather than the transverse electric field of the dipole.

Since the distance z_c is very large for a highly conducting wire, it is desirable for applications to study the properties of the current much closer to the source. In the region $z_d \ll z \ll 1/\kappa_m$, the space-wave current can be written [by combining (142) and (135)] as

$$I_{space}(z) \tilde{=} 2\pi i V_0 \sigma_1 \frac{k_2}{k_1^2} e^{ik_2 z}\left[\frac{1}{\ln[A/(\Gamma z)]} - Q\right] , \qquad (145)$$

where Q is given by (136). The positive number κ_m is the smallest value of κ for which the term Wk_2 in the denominator in (143) can be neglected. The first term on the right-hand side of (145) gives the current that would result if the wire were a perfect conductor. The second term gives the change introduced by the finite conductivity of the wire. It tends to zero as $\sigma_1 \to \infty$. Moreover, Q is nearly independent of z for $z \ll 1/\kappa_m$. Hence, $I_{space}(z)$ differs from the perfect-conductor current distribution by having a component that does not fall off due to geometrical spreading of the space wave in this region.

The primary difference between the current distributions due to the principal mode and the space wave is that the variation of the modal current with z is determined by only its wavenumber h_0 whereas the space-wave current varies with wavenumber k_2 with an additional fall off in amplitude due to geometrical spreading of the space wave. Since h_0 has slightly larger imaginary part than k_2, the space-wave current will always dominate the modal current for very large z. Closer to the source,

however, both currents can be important. Since h_0 is very nearly equal to k_2 and since the geometrical fall-off of the space wave is very slow in the near region, the variation of the currents with z can be nearly the same. The ratio of the amplitudes of the two current is approximated by

$$\left| \frac{I_{space}}{I_{mode}} \right| \tilde{=} \left| [\ln(A\delta)+1] \left[\frac{1}{\ln[A/(\Gamma z)]} - Q \right] \right| e^{-\delta'' z} \qquad (146)$$

for $z_d << z << 1/\kappa_m$.

4.2 NUMERICAL RESULTS

In order to obtain more details concerning the current distribution along the wire and to check the approximations, it is necessary to evaluate $I_{mode}(z)$ and $I_{space}(z)$ numerically. The first is computed from (141) once h_0 has been determined by solving numerically an approximate form of the model equation that is valid for the principal mode. When we apply the approximation $\alpha_1 \tilde{=} k_1$ and the small argument approximations of the Hankel functions in (42), the modal equation (43) reduces to

$$Wk_2^2 + i\alpha_2^2 a k_1 \ln\left(\frac{\Gamma\alpha_2 a}{2i}\right) = 0 \ . \qquad (147)$$

This reduces to the equation treated by Sommerfeld to study the modes of a wire if W is taken to be one. Unfortunately, the numerical procedure applied by Sommerfeld to solve (147) does not converge for parameter values of interest in EMP problems when the correct value of W is applied. Consequently, we applied Muller's method [17] to solve (147) numerically for α_2. Then δ was evaluated by

$$\delta \tilde{=} -\frac{\alpha_2^2}{2k_2} \qquad (148)$$

according to (140) and the equation just above it.

$I_{space}(z)$ was computed numerically from (143) by using the trapezoidal rule to evaluate the integral. The approximations of $I_{space}(z)$ given in (144) and (145) also were evaluated numerically and compared with the value obtained from (143). In order to apply (145), Q given by (136) was computed using the trapezoidal rule. κ_m was taken to be the value of κ at which the error in approximating the integrand in (143) (by neglecting the term Wk_2) is 0.1% of the true integrand.

The values of the parameters used for the computations are presented in Table 1. The wire parameters correspond to a copper wire with resistance of $R = 10^{-3}$ ohm/m. Additional computations were made for $a=7.4403119 \times 10^{-3}$m and $a = 7.4403119 \times 10^{-4}$m which correspond to $R = 10^{-4}$ ohm/m and $R = 10^{-2}$ ohm/m respectively. Since the wire conductivity is so high, the term involving ε_1 in the expressions (3) and (4) for k_1 was neglected.

Table 1. Parameters used in the computations.

$\sigma_1 = 5.75 \times 10^7$ mho/m

$\sigma_2 = 10^{-3}$ mho/m

$\varepsilon_2 = 2000\ \varepsilon_0$

$\omega = 10^3 s^{-1}$

$a = 2.3528332 \times 10^{-3}$m

When the modal equation was solved, it was found that the pole corresponding to the principal mode lies on the lower Riemann sheet for all three values of a. This means that the residue of the pole does not contribute to the current since the sum in (138) is the sum of the

residues of the poles in the upper half of the complex h plane on the upper Riemann sheet. Consequently, we have

$$I_{mode} = 0 \tag{149}$$

for these cases.

It was found by increasing the frequency in the $R = 10^{-3}$ ohms/m case that the pole crosses the branch cut onto the upper Riemann sheet when ω reaches 2.60×10^{4} s^{-1}. At that frequency, the pole begins to contribute an amount given by

$$I_{mode}(z) = - V_0(.033+.025i)e^{ik_2 z} \tag{150}$$

amps at $z = 1000$m. As the pole crosses the branch cut, the branch-cut integral increases abruptly by minus the amount given in (150) so that the total current does not change discontinuously.

Computations also were made for $\sigma_1 = 5.75 \times 10^{12}$ mho/m to see if the results agreed with the asymptotic theory of a perfectly conducting wire. Agreement was found to at least three significant figures for z less than about 10,000 m. Beyond that distance, the perfect-conductor theory begins to break down for this value of σ_1.

In order to display the numerical results, it is convenient to factor out the propagation term $\exp(ik_2 z)$ and the strength V_0 of the excitation. Hence, Figures 3 and 4 respectively show the real and imaginary parts of $I_0(z)$ defined by

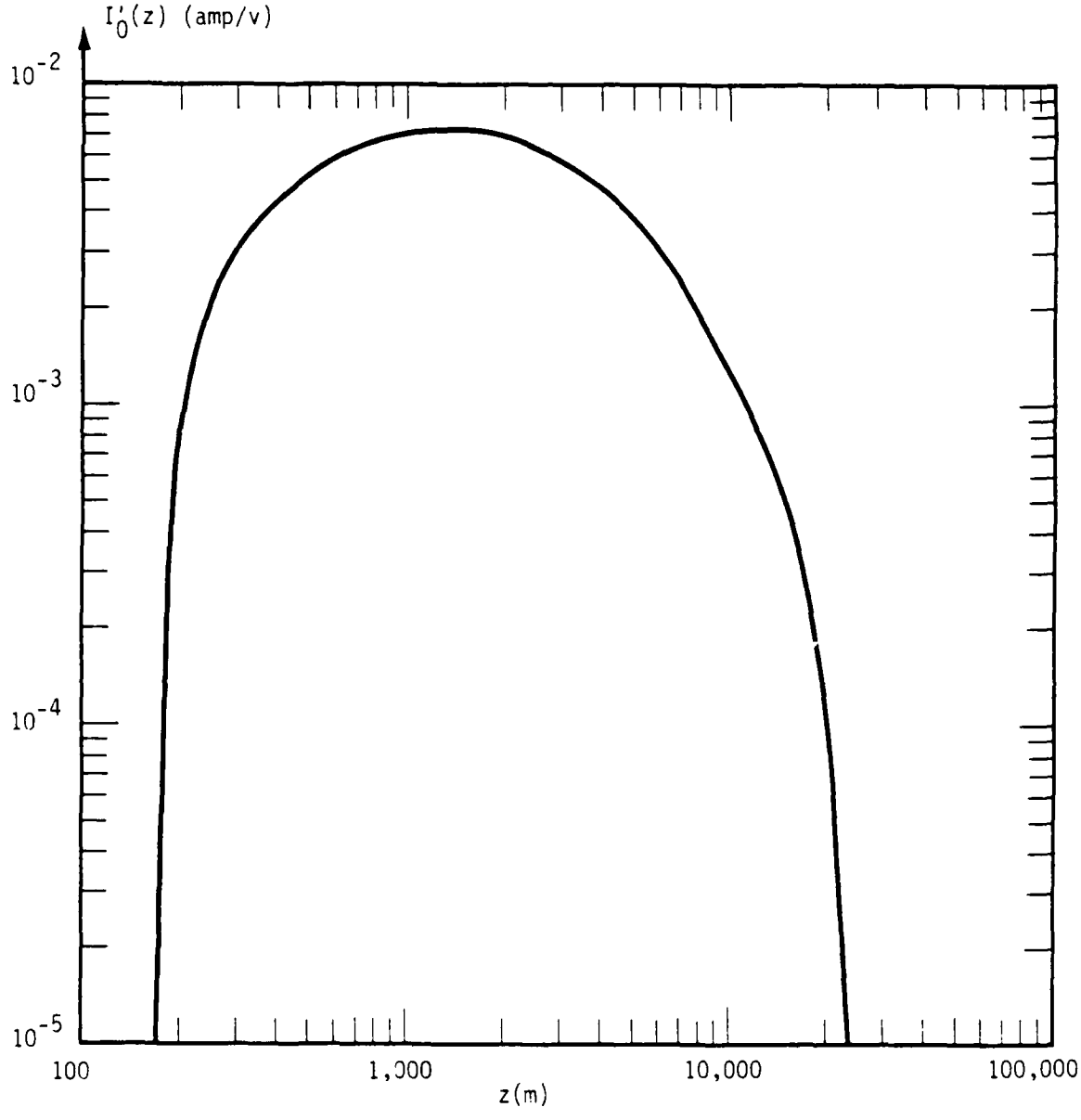

Figure 3. Real part of $I_0(z)$ for $R=10^{-3}$ ohm/m.

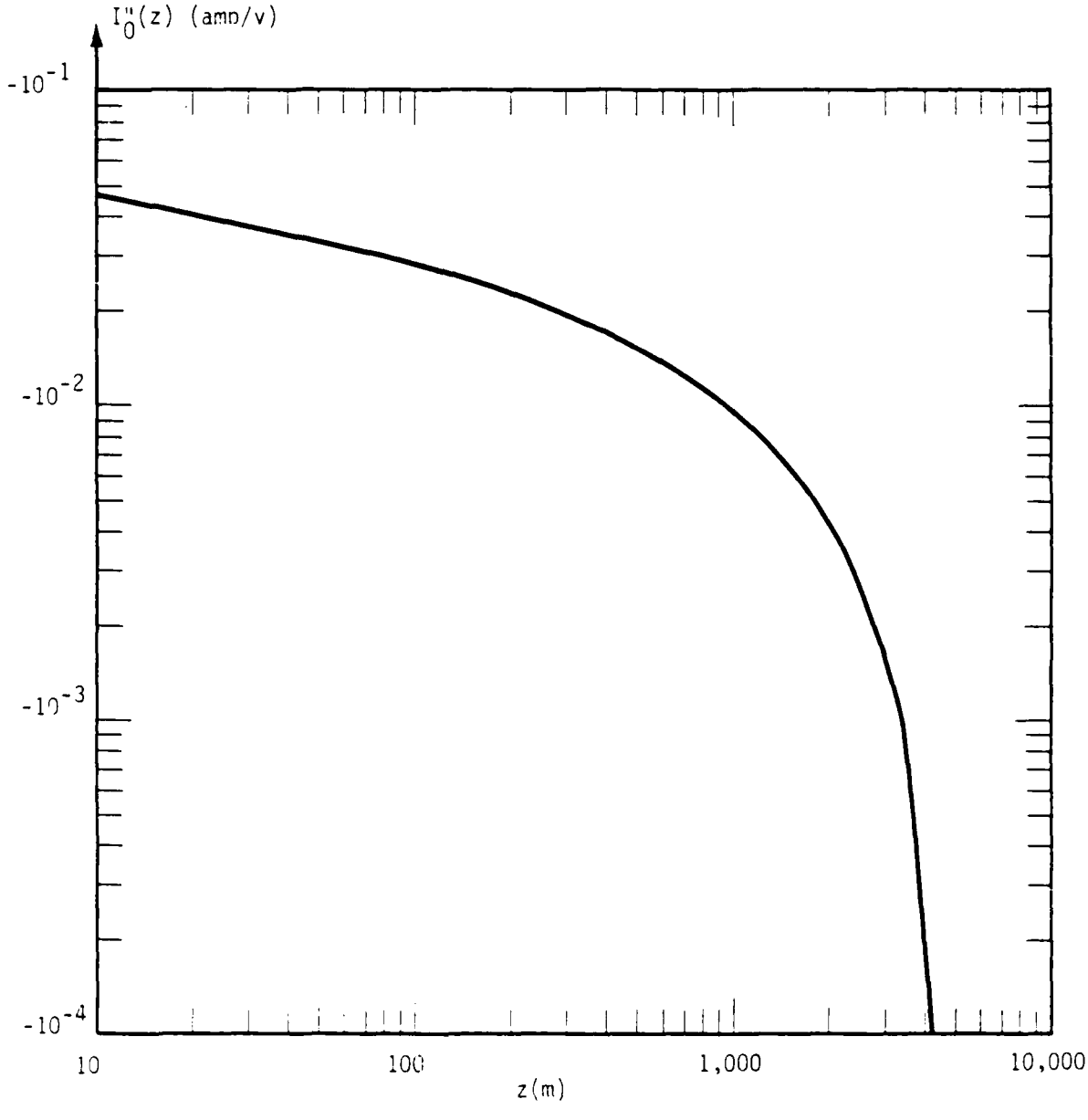

Figure 4. Imaginary part of $I_0(z)$ for $R=10^{-3}$ ohm/m.

$$I_0(z) = \frac{I(z)}{V_0} e^{-ik_2 z} \tag{151}$$

plotted as a function of z on a log-log plot for the parameter values given in Table 1 ($R = 10^{-3}$ ohm/m).

The data shown in these figures do not agree with either of the approximations of $I_{space}(z)$ presented in (144) and (145). To see why, we now determine numerically the regions of validity of the approximations. Both approximations require that $z \gg z_d$ in order for the small-argument approximations of the Hankel functions to be applicable. Evaluation of (97) for the $R = 10^{-3}$ ohm/m case shows that $z_d = 1.2 \times 10^{-8}$ m. Since this value is so small, we conclude that the above condition will be satisfied for any point of interest along the wire.

The other conditions for validity of the approximations are much more restrictive. In particular, in order for (145) to be valid with Q defined by (136) we require that $z \ll 1/\kappa_m$. Numerical computation of the terms in the denominator of the integrand shows that $\kappa_m = 0.83\ m^{-1}$ for the $R = 10^{-3}$ ohm/m case. (See the second paragraph above Table 1 for the definition of κ_m). This means that we require that $z \ll 1.2$ m in order for (145) to be useful. Numerical evaluation of the integral expression for $I_{space}(z)$ and Q for very small z shows that (145) agrees with the true value of $I_{space}(z)$ to within 2 percent for $z < 0.1$ m. Hence, the approximation provides a useful check of our numerical evaluation of the integral but it does not provide an analytic approximation of $I_{space}(z)$ in a region of interest.

Similarly, in order for (144) to be useful, we must have $z \gg z_c = (h'' - k'')^{-1}$. For the $R = 10^{-3}$ ohm/m case, it is found that $z_c = 7.3 \times 10^3$ m. Numerical evaluation of the integral expression for $I_{space}(z)$ shows that the approximation given in (144) is good to within

23 percent for z>10,000 m and to within 3.5 percent for $z>10^6$ m. Again, we find that the approximation provides a valuable check on the numerical evaluation of the integral for $I_{space}(z)$ but it does not provide an analytic expression that is useful in the region of interest along the wire.

The range of validity of the approximations can be better for other values of wire resistance. For $R=10^{-2}$ ohm/m, the value of z_c is found to be 770 m. Comparison of $I_0(z)$ with the approximation corresponding to (144) is shown in Figure 5. It is seen that the approximation is useful for z beyond about 10Km.

For $R=10^{-4}$ ohm/m, κ_m is found to be 0.069 m^{-1}. Hence, (145) is useful for $z<<14.5$ m. Figure 6 shows the comparison of the real part of $I_0(z)$ with the approximation corresponding to (145). Agreement is reasonable for z up to about 10 m.

Figure 6 shows also the real part of the asymptotic approximation of $I_0(z)$ for a perfect conductor. The result is rather surprising. Even at very small distances from the source with wire resistance as low as $R=10^{-4}$ ohm/m, the perfect-conductor result is not very useful. The reason for the difference is easily seen by comparing the numerical values of the integrands in the expressions for $I_{space}(z)$ for the two cases. The absolute values of the integrands are shown in Figure 7 as a function of distance up the branch cut for z=100 m. It is seen that the primary effect of neglecting the finite resistance of the wire is to greatly increase the magnitude of the integrand near the branch point. For the finite resistance case, the integrand is negligible along the portion of the branch cut that is below the pole. For the perfect conductor, however, that portion of the branch cut provides a significant contribution to the integral which increases the absolute value of the resulting current.

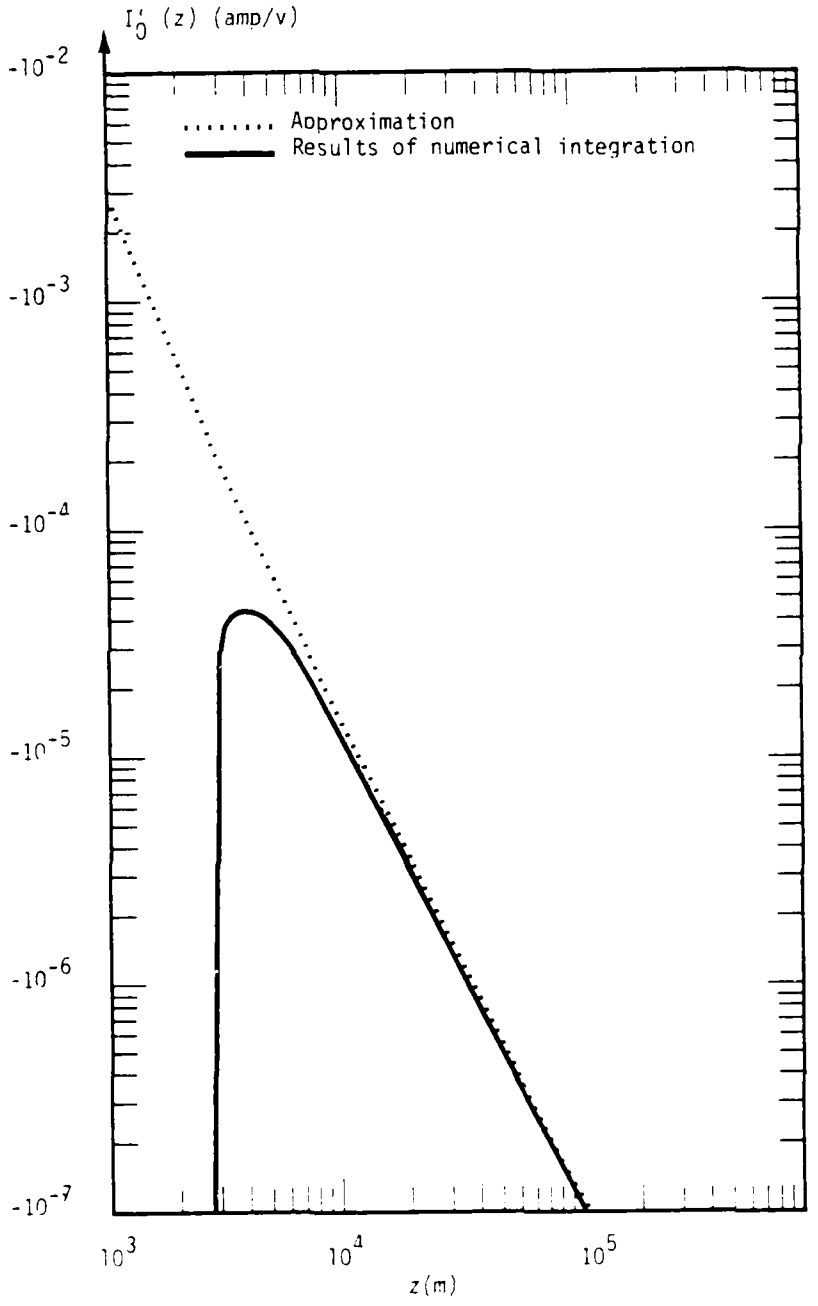

Figure 5. Real part of $I_0(z)$ for $R=10^{-2}$ ohm/m.

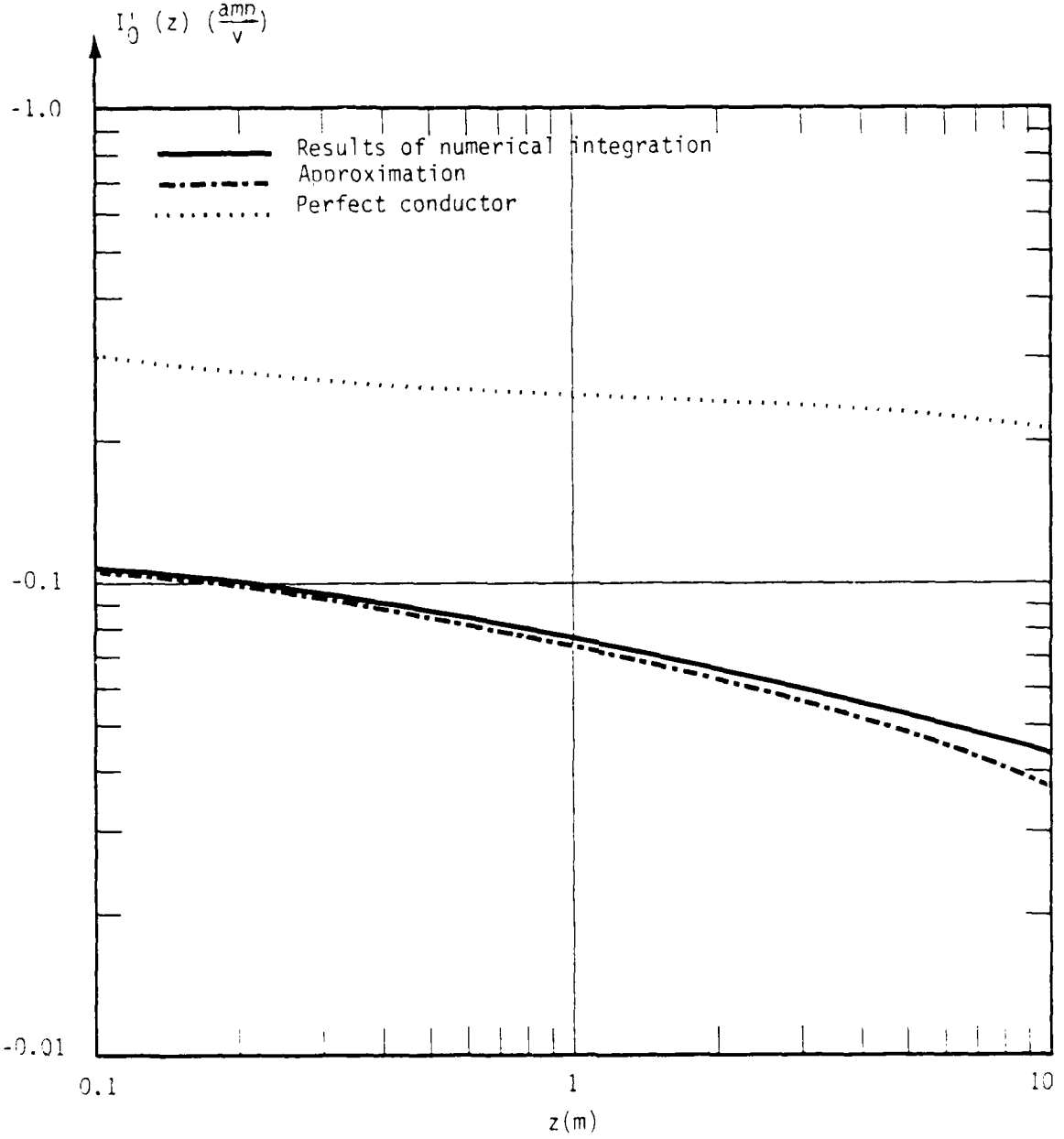

Figure 6. Real part of $I_0(z)$ for $R=10^{-4}$ ohm/m.

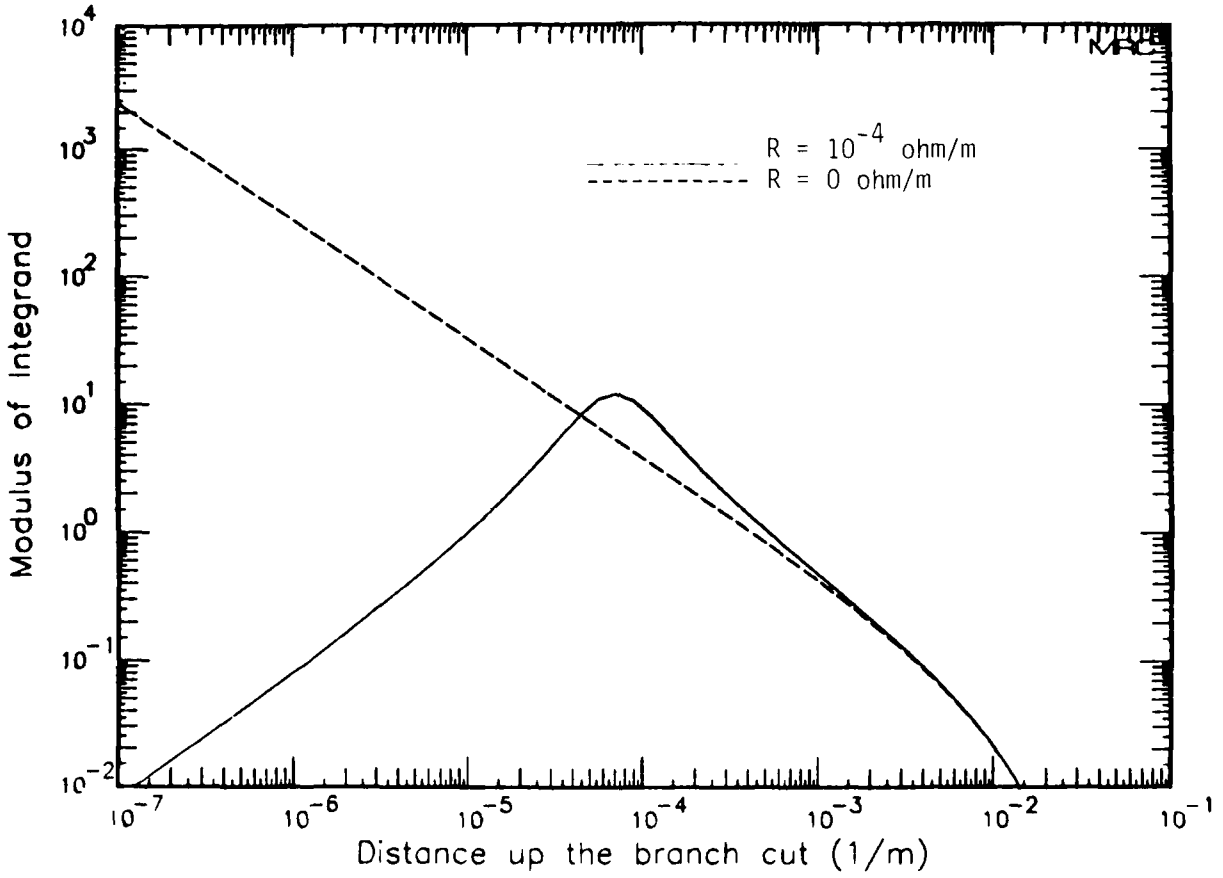

Figure 7. Modulus of the integrand.

In order to display the effect that finite resistance has on the current distribution along the wire, let $I_{PC}(z)$ be the asymptotic approximation of $I_0(z)$ for a perfect conductor defined by

$$I_{PC}(z) = \frac{2\pi i \sigma_1 k_2}{k_2^2 \ln[A/(\Gamma z)]} \tag{152}$$

and let $I_R(z)$ be defined by

$$I_0(z) = I_{PC}(z) + I_R(z) \tag{153}$$

for the resistive wire*. With this definition $I_R(z)$ was determined numerically for the $R=10^{-3}$ ohm/m case by numerical evaluation of $I_0(z)$ and $I_{PC}(z)$. The results are shown in Table 2 where A_0, A_{pc}, A_R and ϕ_0, ϕ_{PC}, ϕ_R are respectively the amplitudes in amp/m and phases in radians of $I_0(z)$, $I_{PC}(z)$, and $I_R(z)$. It is seen that $I_R(z)$ is a very slowly varying function of z over a very large range. Moreover, it is seen that $I_R(z)$ is similar in magnitude to $I_{PC}(z)$ but nearly opposite in phase. As a result, the amplitude of the current is reduced from the perfect-conductor case by a substantial amount which is given the last column in Table 2. The results show that the decrease in current amplitude is nearly independent of distance from the source over the entire range of interest. Since the current in a perfect conductor decreases with distance from the source, the relative change in current due to wire resistance increases with distance.

---

* Note that for $z_d << z << 1/\kappa_m$, $I_R(z)$ is approximately proportional to Q according to (145).

Table 2. Change in current due to wire resistance of 10^{-3} ohm/m.

z(m)	$I_0(z)$		$I_{PC}(z)$		$I_R(z)$		$A_{PC} - A_0$
	A_0	ϕ_0	A_{PC}	ϕ_{PC}	A_R	ϕ_R	
10^0	.0816	1.31π	.295	1.23π	.216	$.206\pi$	.213
10^1	.0517	1.36π	.263	1.24π	.216	$.207\pi$	.211
10^2	.0288	1.21π	.237	1.24π	.216	$.209\pi$	.208
10^3	.0119	$-.299\pi$	.217	1.24π	.215	$.220\pi$	.205
10^4	.00175	$.247\pi$	.198	1.24π	.215	$.238\pi$	.196

SECTION 5
CONCLUSIONS

The results of this study have exposed the reason that transmission-line theory does not describe accurately the behavior of currents generated by localized sources on uninsulated wires. The current is dominated by an electromagnetic space wave that radiates energy out into space. Since transmission-line theory applies to TEM modes guided by the transmission line, it does not describe the behavior of space waves. Although the wire does support a guided TM mode that is approximately transverse electric and hence, could be described by transmission-line theory, the frequencies of interest are too low for the mode to be excited. For frequencies above several KHz, the mode begins to be excited but it still makes only a minor contribution to the total current.

A simple analytic approximation is available for the current distribution along the wire in the region of interest provided that the wire is a perfect conductor. This study has provided the numerical values of the correction term that must be added to account for the finite resistance of the wire for typical conductivities. It was found that the correction term is nearly constant along the wire and that it is similar in magnitude but nearly opposite in phase from the perfect-conductor result. Consequently, an important effect of finite wire resistance is to reduce the current amplitude by a substantial amount that is nearly independent of distance from the source. The relative difference in the current, however, increases with distance from the source. For $R=10^{-3}$ ohm/m, the current amplitude is about 20 percent of the perfect-conductor result for z=1m and about 5 percent for z=1000m.

REFERENCES

1. D. R. Marston and W. R. Graham, "Currents induced in cables in the Earth by a continuous-wave electromagnetic field," Electromagnetic Pulse Interaction Notes Vol 2, C. E. Baum, ed. Note 24.

2. H. J. Price and D. E. Stevenson, "Notes on planar, cylindrical electromagnetic waves and propagation on circularly-symmetric transmission lines," ibid. Note 26.

3 J. Dancz and J. Gilbert, Special Study Phase 2 - SREMP Coupling to Long Lines, Mission Research Corporation, unpublished.

4. S.W. Lee and R. Mittra, "Admittance of a solid cylindrical antenna," Canadian J. Phys. 47, 1959-1970 (1969).

5. J.R. Wait, "Electromagnetic Surface Waves" in Advances in Radio Research, Vol. 1, J.A. Saxton, ed. (Academic Press, London, 1964). pp. 157-217.

6. J.R. Wait and D.A. Hill, "Theory of Transmission of Electromagnetic Waves Along a Drill Rod in Conducting Rock," IEEE Trans. Geoscience Electronics GE-17, 21-24(1979).

7. J.A. Stratton, Electromagnetic Theory (McGraw-Hill Book Co., Inc., New York 1941). Chap. I, Sec. 1.11.

8. M. Abramowitz and I.A. Stegun, Handbook of Mathematical Functions (Dover Publications, Inc., New York 1965). Chap. 9.

9. Ref. 8, § 9.1.16 on p. 360 combined with §9.1.3 on p. 358.

10. I.S. Gradshteyn and I.M. Ryzhik, Tables of Integrals, Series and Products, 4th ed. (Academic Press, New York, 1965) p. 634, §5.52

11. A. Hessel, "General Characteristics of Traveling - Wave Antennas" in Antenna Theory, R.E. Collin and F.J. Zucker, eds. (McGraw-Hill Book Co., N.Y. 1963) pp. 151-258.

12. E.T. Whittaker and G.N. Watson, A Course in Modern Analysis (Cambridge at the University Press, Fourth ed., 1963). Chap. 6.

13. Ruel V. Churchill, Introduction to Complex Variables and Applications, (McGraw Hill, N.Y., 1948). Sec. 69.

14. Ref. 7, Sec. 9.16.

15. Max Born and Emil Wolf, Principles of Optics (Pergamon Press, Oxford, 4th ed., 1970). Sec. 2.2.3.

16. Ref. 8, p 229.

17. S.D. Conte and Carlde Boor, Elementary Numerical Analysis (McGraw-Hill Book Co., New York, 3rd ed., 1980). Sec. 3.6.

DISTRIBUTION LIST

DEPARTMENT OF DEFENSE

Asst to the Secretary of Defense
Atomic Energy
ATTN: Executive Assistant
ATTN: J. Rubell

Defense Communications Agency
ATTN: Code C313

Defense Communications Engineer Center
ATTN: Code R720, C. Stansberry
ATTN: Code R123, Tech Library
ATTN: Code R400

Defense Intelligence Agency
ATTN: DB-4C
ATTN: RTS-2A, Tech Library
ATTN: DB 4C2, D. Spohn

Defense Nuclear Agency
ATTN: RAEV
ATTN: NASF
ATTN: STNA
ATTN: RAEE
4 cy ATTN: STTI-CA

Defense Technical Information Center
12 cy ATTN: DD

Field Command, DNA, Det 1
Lawrence Livermore National Lab
ATTN: FC-1

DNA PACOM Liaison Office
ATTN: J. Bartlett

Field Command, DNA
ATTN: FCLMC, H. Putnam
ATTN: FCPR
ATTN: FCTXE
ATTN: FCTT, W. Summa

Interservice Nuclear Weapons School
ATTN: TTV

Joint Chiefs of Staff
ATTN: J-3, Strat Ops Division

Joint Strat Tgt Planning Staff
ATTN: JPSS
ATTN: JPTM
ATTN: JLAA
ATTN: JLKC
ATTN: JLKS
ATTN: JLK, DNA Rep
3 cy ATTN: JPPFD

National Communications System
ATTN: NCS-TS

National Security Agency
ATTN: R-52, O. Van Gunten
ATTN: Chief A Group, J. Amato
ATTN: R52

DEPARTMENT OF DEFENSE (Continued)

Under Secy of Def for Rsch & Engrg
ATTN: Strat & Space Sys (OS)
ATTN: Strat & Theater Nuc For, B. Stephan

DEPARTMENT OF THE ARMY

BMD Advanced Technology Center
ATTN: ATC-T
ATTN: ATC-R

BMD Systems Command
ATTN: BMDSC-HW

Harry Diamond Laboratories
ATTN: DELHD-TD
ATTN: DELHD-NW-P
ATTN: Chief Div 10000
ATTN: DELHD-TF
ATTN: DELHD-TA-L, Tech Lib
ATTN: DELHD-NW-EC
ATTN: DELHD-NW-EA
ATTN: DELHD-NW-EE
ATTN: 00100 Commander, Tech Dir/Div Dir
ATTN: DELHD-NW-EB
ATTN: DELHD-NW-ED
ATTN: DELHD-NW-E
ATTN: DELHD-?
ATTN: DELHD-NW, J. Bombardt

Research & Dev Center
ATTN: DRCPM-ATC
ATTN: DRDCO-SEI

US Army Armor Center
ATTN: Tech Library

US Army Ballistic Research Labs
ATTN: DRDAR-BLE
ATTN: DRDAR-BLA-S, Tech Library

US Army Comm-Elec Engrg Instal Agency
ATTN: CCC-CED-SES

US Army Communications Command
ATTN: CC-OPS-OS
ATTN: CC-OC-SAP
ATTN: CC-ENGR
ATTN: CC-OPS-PD
ATTN: ATSI-CD-MD

US Army Communications Sys Agency
ATTN: CCM-RD-T
ATTN: CCM-AD-SV

US Army Electronics R&D Command
ATTN: DELSD-L, W. Werk

US Army Engineer Div Huntsville
ATTN: HNDED-SR
ATTN: T. Bolt

US Army Intel Threat Analysis Det
ATTN: Admin Officer

DEPARTMENT OF THE ARMY (Continued)

US Army Intelligence & Sec Command
ATTN: Technical Library
ATTN: Tech Info Fac

US Army Materiel Sys Analysis Actvy
ATTN: DRXSY-CC
ATTN: DRXSY-PO

US Army Test and Evaluation Comd
ATTN: DRSTE-CT-C
ATTN: DRSTE-CM-F

US Army Training and Doctrine Comd
ATTN: ATCD-Z

US Army White Sands Missile Range
ATTN: STEWS-TE-N, K. Cummings

USA Missile Command
ATTN: DRSMI-SF, G. Thurlow
ATTN: Documents Section
ATTN: DRCPM-PE-EA, W. Wagner
ATTN: DRCPM-PE-EG, W. Johnson

DEPARTMENT OF THE NAVY

Naval Air Systems Command
ATTN: AIR 350F

Naval Electronic Systems Command
ATTN: PME 117-21

Naval Intelligence Support Center
ATTN: Code 41

Naval Ocean Systems Center
ATTN: Code 7309, R. Greenwell

Naval Ordance Station
ATTN: Standardization Division

Naval Postgraduate School
ATTN: Code 1424, Library

Naval Research Laboratory
ATTN: Code 2627, D. Folen
ATTN: Code 1434, E. Brancato
ATTN: Code 6624

Naval Surface Weapons Center
ATTN: Code F30
ATTN: Code F32, E. Rathbun

Naval Surface Weapons Center
ATTN: Code F-56

Naval Weapons Center
ATTN: Code 343, Tech Svcs

Naval Weapons Evaluation Facility
ATTN: Code AT-6

Strategic Systems Project Office
ATTN: NSP-2301, M. Meserole
ATTN: NSP-2342, R. Coleman
ATTN: NSP-43, Tech Library
ATTN: NSP-2701
ATTN: NSP-27334

DEPARTMENT OF THE NAVY (Continued)

Ofc of the Deputy Chief of Naval Ops
ATTN: NOP 981N1
ATTN: NOP 981

DEPARTMENT OF THE AIR FORCE

Aeronautical Systems Division
ATTN: ASD/ENESS, P. Marth
ATTN: ASD/YYEF
ATTN: ASD/ENSSA

Air Force Aeronautical Sys Division
ATTN: ASD/ENACE, J. Corbin

Air Force Weapons Laboratory
ATTN: CA
ATTN: NTYEE, C. Baum
ATTN: NTYEP, W. Page
ATTN: NT
ATTN: SUL
ATTN: NTN
ATTN: NTYC, M. Schneider

Air Logistics Command
ATTN: OO-ALC/MMETH, P. Berthel
ATTN: OO-ALC/MMEDO, L. Kidman
ATTN: OO-ALC/MM

Air University Library
ATTN: AUL-LSE

Ballistic Missile Office
ATTN: ENSN, W. Wilson
ATTN: ENSN, W. Clark

Electronic Systems Division
ATTN: SCS-1E

Foreign Technology Division
ATTN: NIIS, Library
ATTN: TQTD, B. Ballard

Rome Air Development Center
ATTN: TSLD

Sacramento Air Logistics Center
ATTN: MMCREB, F. Schrader
ATTN: MMEAE, R. Dallinger

Space Command
ATTN: DEE

Space Division
ATTN: IND

Space Division
ATTN: YKM

Strategic Air Command
ATTN: DCX
ATTN: DCZ
ATTN: DEMUE
ATTN: DEPM
ATTN: DOCSD
ATTN: NRI, STINFO Library
ATTN: INAO
ATTN: XPFC
ATTN: XPFS
ATTN: XPQ

DEPARTMENT OF THE AIR FORCE (Continued)

AFIT/ENA
ATTN: G. Baker

DEPARTMENT OF ENERGY

Department of Energy
Albuquerque Operations Office
ATTN: WSSB
ATTN: CTID

Department of Energy
Emergency Electric Power Adm
ATTN: L. O'Neill

OTHER GOVERNMENT AGENCIES

US Department of State
ATTN: PM/STM

Central Intelligence Agency
ATTN: OSWR/NED
ATTN: OSWR/STD/MTB

Department of Transportation
ATTN: Sec Div ASE-300

Federal Emergency Management Agency
ATTN: SL-EM, J. Hain
ATTN: OPIR, M. Murtha

Norad
ATTN: J5YX

DEPARTMENT OF ENERGY CONTRACTORS

University of California
Lawrence Livermore National Lab
ATTN: L-10, H. Kruger
ATTN: L-156, H. Cabayan
ATTN: L-97, T. Donich
ATTN: Technical Info Dept Library

Los Alamos National Laboratory
ATTN: B. Noel
ATTN: MS670, J. Malik

Sandia National Laboratories
ATTN: Org 2322, E. Hartman
ATTN: M. Morris

DEPARTMENT OF DEFENSE CONTRACTORS

Aerospace Corp
ATTN: I. Garfunkel
ATTN: J. Reinheimer
ATTN: Library
ATTN: C. Greenhow

Agbabian Associates
ATTN: Library

Allied Corp
ATTN: Document Control

American Telephone & Telegraph Co
ATTN: W. Edwards

AVCO Systems Division
ATTN: Library

DEPARTMENT OF DEFENSE CONTRACTORS Continued)

Battelle Memorial Institute
ATTN: E. Leach

BDM Corp
ATTN: Corporate Library

BDM Corp
ATTN: Library
ATTN: J. Schwarz

Bendix Corp
ATTN: Dept 6401

Boeing Co
ATTN: D. Kemle
ATTN: D. Egelkrout
ATTN: H. Wicklein
ATTN: Kent Technical Library
ATTN: J. Dicome

Boeing Military Airplane Co
ATTN: C. Sutter

Booz-Allen & Hamilton, Inc
ATTN: R. Chrisner
ATTN: Technical Library

Brunswick Corp
ATTN: R. White

Calspan Corp
ATTN: Library

Charles Stark Draper Lab, Inc
ATTN: K. Fertig
ATTN: TIC MS 74

Cincinnati Electronics Corp
ATTN: C. Stump
ATTN: L. Hammond

Computer Sciences Corp
ATTN: A. Schiff

Dikewood Corp
ATTN: Tech Lib For D. Pirio
ATTN: Technical Library
ATTN: Tech Lib for C. Jones

E-Systems, Inc
ATTN: J. Moore

Eaton Corp
ATTN: E. Karpen

EG&G Wash Analytical Svcs Center, Inc
ATTN: C. Giles

Electro-Magnetic Applications, Inc
ATTN: D. Merewether

Emerson & Cuming, Inc
ATTN: J. Flaherty

Ford Aerospace & Communications Corp
ATTN: H. Linder

Franklin Institute
ATTN: R. Thompson

DEPARTMENT OF DEFENSE CONTRACTORS (Continued)

General Dynamics Corp
ATTN: Research Library

General Dynamics Corp
ATTN: Research Library

General Electric Co
ATTN: J. Andrews

General Electric Co
ATTN: C. Hewison

General Electric Co
ATTN: Technical Library

General Research Corp
3 cy ATTN: Technical Info Office

Georgia Institute of Technology
ATTN: Res & Sec Coord for H. Denny

Grumman Aerospace Corp
ATTN: L-01 35

GTE Communications Products Corp
ATTN: J. McElroy

GTE Communications Products Corp
ATTN: H. Gelman
ATTN: J. Waldron
ATTN: A. Murphy
ATTN: D. Flood
ATTN: M. Snow
ATTN: F. Hammond

GTE Government Systems Corp
ATTN: L. Lesinski
ATTN: R. Steinhoff

Harris Corp
ATTN: A. Strain
ATTN: V Pres & Mgr Prgms Div

Hazeltine Corp
ATTN: J. Okrent

Honeywell, Inc
ATTN: R. Johnson
ATTN: S&RC Library

Honeywell, Inc
ATTN: S. Grafe
ATTN: W. Stewart

Hughes Aircraft Co
ATTN: A. Narevsky

Hughes Aircraft Co
ATTN: K. Walker
ATTN: CTDC 6/E110

IIT Research Institute
ATTN: I. Mindel
ATTN: J. Bridges

Institute for Defense Analyses
ATTN: Tech Info Services

DEPARTMENT OF DEFENSE CONTRACTORS (Continued)

IRT Corp
ATTN: B. Williams
ATTN: N. Rudie

ITT Corp
ATTN: A. Richardson
ATTN: Technical Library

JAYCOR
ATTN: W. Radasky
ATTN: D. Higgins

JAYCOR
ATTN: R. Poll
ATTN: R. Schaefer

JAYCOR
ATTN: Library

JAYCOR
ATTN: E. Wenaas
ATTN: R. Stahl

Johns Hopkins University
ATTN: P. Partridge

Kaman Sciences Corp
ATTN: A. Bridges
ATTN: F. Shelton
ATTN: W. Rich
ATTN: N. Beauchamp

Kaman Sciences Corp
ATTN: E. Conrad

Kaman Tempo
ATTN: DASIAC

Kaman Tempo
ATTN: DASIAC
ATTN: W. Hobbs
ATTN: R. Rutherford
ATTN: W. McNamara

Litton Systems, Inc
ATTN: MS 64-61, E. Eustis

Litton Systems, Inc
ATTN: J. Skaggs

Litton Systems, Inc
ATTN: J. Moyer

Lockheed Missiles & Space Co, Inc
ATTN: B. Kimura
ATTN: L. Rossi
ATTN: S. Taimuty
ATTN: H. Thayn
ATTN: D. Nishida

Lockheed Missiles & Space Co, Inc
ATTN: Technical Info Center

Lutech, Inc
ATTN: F. Tesche

Magnavox Govt & Indus Electronics Co
ATTN: W. Richeson

DEPARTMENT OF DEFENSE CONTRACTORS (Continued)

Martin Marietta Corp
ATTN: M. Griffith
ATTN: J. Casalese

McDonnell Douglas Corp
ATTN: M. Potter
ATTN: W. McCloud

McDonnell Douglas Corp
ATTN: S. Schneider
ATTN: Tech Library Services

McDonnell Douglas Corp
ATTN: T. Ender

Metatech Corp
ATTN: W. Radasky

Mission Research Corp
ATTN: C. Longmire
ATTN: EMP Group
2 cy ATTN: G. Sherman
5 cy ATTN: Document Control

Mission Research Corp
ATTN: M. Scales
ATTN: A. Chodorow

Mission Research Corp
ATTN: W. Stark
ATTN: J. Lubell
ATTN: W. Ware

Mitre Corp
ATTN: M. Fitzgerald

Norden Systems, Inc
ATTN: Technical Library
ATTN: D. Longo

Northrop Corp
ATTN: Rad Effects Grp

Pacific-Sierra Research Corp
ATTN: H. Brode, Chairman SAGE

Palisades Inst for Rsch Services, Inc
ATTN: Records Supervisor

Physics International Co
ATTN: Document Control

R&D Associates
ATTN: Document Control
ATTN: C. Knowles
ATTN: W. Karzas
ATTN: C. Mo
ATTN: P. Haas

Rand Corp
ATTN: Lib-D
ATTN: P. Davis

Rand Corp
ATTN: B. Bennett

Raytheon Co
ATTN: H. Flescher
ATTN: M. Nucefora
ATTN: B. Schupp

DEPARTMENT OF DEFENSE CONTRACTORS (Continued)

RCA Corp
ATTN: D. O'Connor
ATTN: L. Minich

RCA Corp
ATTN: G. Brucker

Rockwell International Corp
ATTN: N. Rudie
ATTN: J. Erb
ATTN: V. Michel
ATTN: D/243-068, 031-CA31
ATTN: G. Morgan

Rockwell International Corp
ATTN: B-1 Div Tic, BA0B

Rockwell International Corp
ATTN: F. Shaw

Rockwell International Corp
ATTN: B. White

Sanders Associates, Inc
ATTN: R. Despathy

Science & Engrg Associates, Inc
ATTN: V. Jones

Science Applications Intl Corp
ATTN: E. Parkinson

Science Applications, Inc
ATTN: E. O'Donnell

Science Applications, Inc
ATTN: W. Chadsey

Sidney Frankel & Associates
ATTN: S. Frankel

Singer Co
ATTN: Technical Info Center

Sperry Corp
ATTN: Technical Library

Sperry Corp
ATTN: M. Cort

Sperry Flight Systems
ATTN: D. Schow

SRI International
ATTN: A. Padgett

SRI International
ATTN: A. Whitson
ATTN: M. Tarrasch

Teledyne Brown Engineering
ATTN: F. Leopard
ATTN: J. Whitt

Texas Instruments, Inc
ATTN: D. Manus
ATTN: Technical Library

Transients Limited Corp
ATTN: D. Clark

DEPARTMENT OF DEFENSE CONTRACTORS (Continued)

TRW Electronics & Defense Sector
ATTN: O. Adams
ATTN: H. Holloway
ATTN: R. Plebuch
ATTN: W. Gargaro

Raytheon Co.
ATTN: G. Joshi

DEPARTMENT OF DEFENSE CONTRACTORS (Continued)

TRW Electronics & Defense Sector
ATTN: R. Kitter
ATTN: R. Mortensen

United Technologies Corp
ATTN: Chief Elec Design